ARTIFICIAL NEURAL NETWORKS MODELING AND SIMULATION OF THE IN-VITRO NANOPARTICLES - CELL INTERACTIONS

A THESIS

SUBMITTED TO THE DEPARTMENT OF INDUSTRIAL ENGINEERING

AND THE GRADUATE SCHOOL OF ENGINEERING AND SCIENCE

OF BILKENT UNIVERSITY

IN PARTIAL FULFILLMENT OF THE REQUIREMENTS

FOR THE DEGREE OF

MASTER OF SCIENCE

By

Neslihan Cenk

January, 2012

I certify that I have read this thesis and that in my opinion it is fully adequate, in scope and in quality, as a thesis for the degree of Master of Science.

_____

Prof. Dr. İhsan Sabuncuoğlu

I certify that I have read this thesis and that in my opinion it is fully adequate, in scope and in quality, as a thesis for the degree of Master of Science.

_____

Assoc. Prof. Dr. Savaş Dayanık

I certify that I have read this thesis and that in my opinion it is fully adequate, in scope and in quality, as a thesis for the degree of Master of Science.

_____

Assoc. Prof. Dr. Oya Karasan

I certify that I have read this thesis and that in my opinion it is fully adequate, in scope and in quality, as a thesis for the degree of Master of Science.

_____

Assist. Prof. Dr. Gürer Budak

Approved for the Graduate School of Engineering and Science:

_____

Prof. Dr. Levent Onural
Director of the Graduate School

ABSTRACT

ARTIFICIAL NEURAL NETWORKS MODELING AND SIMULATION OF THE IN-VITRO NANOPARTICLE-CELL INTERACTIONS

Neslihan Cenk
M.S. in Industrial Engineering
Supervisor: Prof. Dr. İhsan Sabuncuoğlu
Co-Supervisor: Assoc. Prof. Dr. Savaş Dayanık
January, 2012

In this research a prediction model for cellular uptake efficiency of nanoparticles (NPs), which is the rate of NPs adhered to the cell surface or entered into the cell, is investigated via Artificial Neural Network (ANN) method. Prediction of cellular uptake rate of NPs is an important study considering the technical limitations of volatile environment of organism and the time limitation of conducting numerous experiments for thousands of possible variations of different variables that have an impact on NP uptake rate. Moreover, this study constitutes a basis for the targeted drug delivery and cell-level detection, treatment and diagnoses of existing pathologies through simulating experimental procedure of NP-Cell interactions. Accordingly, this study will accelerate nano-medicine researches. The research focuses on constructing a proper ANN model based on multilayered feed-forward back-propagation algorithm for prediction of cellular uptake efficiency which depends on NP type, NP size, NP surface charge, concentration and time. NP types for in-vitro NP-healthy cell interaction analysis are polymethyl methacrylate

(PMMA), silica and polylactic acid (PLA) all of whose shapes are spheres. The proposed ANN model has been developed on MATLAB Programming Language by optimizing number of hidden layers, node numbers and training functions. The data sets for training and testing of the network are provided through in-vitro NP-cell interaction experiments conducted by a Nano-Medicine Research Center in Turkey. The dispersion characteristics and cell interactions of the different nanoparticles in organisms are explored through constructing and implementing an optimal prediction model using ANNs. Simulating the possible interactions of targeted nanoparticles with cells via ANN model could lead to a more rapid, more convenient and less expensive approach in comparison to numerous experimental variations.

Keywords: Nano-medicine, targeted drug delivery, nanoparticle uptake rate, artificial neural networks, prediction model

ÖZET

YAPAY SİNİR AĞLARI İLE İN-VİTRO NANOPARTİKÜL-HÜCRE ETKİLEŞİMLERİNİN MODELLENMESI VE SİMÜLASYONU

Neslihan Cenk
Endüstri Mühendisliği, Yüksek Lisans
Tez Yöneticisi: Prof. Dr. İhsan Sabuncuoğlu
Yardımcı Tez Yöneticisi: Doç. Dr. Savaş Dayanık
Ocak, 2012

Bu araştırmada, Yapay Sinir Ağları (YSA) yöntemi ile hücreye tutunan, yani hücre yüzeyine yapışan ve hücre içine alınan, nanopartikül (NP) oranını tahmin eden bir model geliştirilmiştir. Organizmaların kaotik ortamları, teknik kısıtlamaları ve tutunma oranına etkisi olan birçok değişkenin binlerce varyasyonunun deneylerle test edilmesinin çok uzun süre gerektireceği göz önünde bulundurulduğunda nanopartiküllerin hücreye tutunma oranının tahmini çok önemli ve gerekli bir çalışmadır. NP-hücre etkileşimleri deney süreçlerinin simülasyonu ile güdümlü ilaç dağılımı, mevcut patolojilerin hücre düzeyinde tespiti, tedavisi ve teşhisi için temel oluşturulmaya çalışılmıştır. Bu çalışma ayni zamanda nanotıp çalışmalarını hızlandıracaktır. NP tipi, NP boyutu, NP yüzey yükü, yoğunluk ve zamana bağlı olan hücresel tutunma oranının tahmini için çok katmanlı, ileri beslemeli, Backpropagation (Geri-Yayılım) algoritmasına dayalı bir YSA modeli geliştirilmiştir. In-vitro NP-sağlıklı hücre etkileşimi analizleri için kullanılacak NP

çeşitlerinin her biri küresel sekle sahip olan polimetil metakrilat (PMMA), silika ve polilaktik asit (PLA) olarak belirlenmiştir. Önerilen YSA modelinde kullanılacak gizli katman sayısı, nöron sayısı ve eğitim fonksiyonlarını optimize etmek için MATLAB Programlama Dili kullanılmıştır. Ağın eğitim ve test edilmesi için gerekli veri seti Türkiye'de bir Nano-Tıp Araştırma Merkezi tarafından yapılan in-vitro NP-hücre etkileşimi deneyleri sonucunda elde edilmiştir. YSA yöntemiyle en iyi tahmin modeli oluşturarak ve uygulayarak farklı nanopartiküllerin dağılım özellikleri ve hücre etkileşimleri incelenmiştir. Birçok farklı deney gerçekleştirmek yerine YSA modeli kullanılarak hücreler ile hedeflenen nanopartiküllerin olası etkileşimlerinin simülasyonu, çok daha hızlı, daha elverişli ve daha ucuz bir yaklaşımdır.

Anahtar Sözcükler: Nano-tıp, güdümlü ilaç dağılımı, hücre içine nanopartikül alım oranı, yapay sinir ağları, tahmin modeli

Acknowledgement

I would like to thank my supervisor, Prof. Dr. Sabuncuoğlu, and my co-supervisers, Asst. Prof. Dr. Dayanık, and Dr. Budak for their guidance and support throughout the course of this research.

Thanks also go to my friends and colleagues and the department faculty and staff for making my time at Bilkent University a great experience.

Finally, thanks to my mother and father for their encouragement throughout my life.

Contents

List of Figures

List of Tables

Chapter 1

Introduction

This thesis aims to predict cellular uptake rate of NPs through an appropriate ANN model by utilizing a limited number of NP-cell interaction data obtained from in-vitro experiments. NP- cell interaction is simulated for 48 hours of incubation period to obtain cellular uptake rate by using an optimized ANN prediction model. The proposed model is used for NP characterization and specifications of desired cellular uptake efficiency without actually conducting numerous experiments. Hence, the results of this research advance NPs synthesis and characterization for targeted drug delivery, diagnosis and imaging systems.

Cellular uptake efficiency depends on variables such as NP size, chemical structure of NPs, NP shape, surface charge and the concentration of NPs. Considering thousands of different values of these variables; it is quite difficult to conduct all the experiments to obtain NP-cell interaction data within the scope of the current technical limitations of NPs. Even if it is technically feasible to produce all the required NPs, it may be impractical or too costly to conduct all experiments in the laboratory conditions. Analyses of biological systems and physiological systems are further complicated due to the fact that living organisms or cells operate in a very

volatile environment. These complex relationships of viable cells can only be modeled accurately with strong statistical tools. Because statistical models that are capable of simulating the possible interactions of targeted nanoparticles with cells could lead to a more rapid, more convenient and less expensive approach in comparison to conducting various experiments. In this study, we use the artificial neural network approach as the modeling and analysis tool.

The ANN approach is preferred over the other statistical tools because they are strong at solving nonlinear complex problems. In general, ANNs are applied in various applications such as function approximation, optimization, classification, forecasting and modeling in order to solve challenging problems. Paliwal et al. (2009) investigated comparative studies on traditional statistical techniques used for prediction and classification purposes in various fields of applications. These statistical techniques are ANNs, discriminant analysis, logistics regression and nonlinear regression analysis. The review reveals that out of 96 comparative studies neural network's performance is better in 56 cases and at least performs as well as other methods in 23 cases. This study highlights the importance of artificial neural networks on the prediction problems. For that reason, we prefer the ANN approach in the NP uptake prediction problem.

Nonlinear NP-cell relationships must be accurately generalized by constructing and implementing a proper ANN model. However, determination of appropriate parameters, functions and structure of network play an essential role to obtain optimal ANN model. Accordingly, an ANN method based on multilayered feed-

forward back-propagation algorithm was built as a forecasting model for the prediction of the cellular uptake rate of NPs which depends on NP type, NP size, NP surface charge, concentration and time. This ANN algorithm has been constructed on MATLAB Programming Language (MATLAB, 2011) and the data for training and testing of the network is provided through in-vitro nanoparticles-cell interaction experiments conducted by Nano-Medicine Research Center in Turkey.

The dispersion characteristics and cell interactions of the nanoparticles in organisms are fundamental and must be investigated in the targeted drug delivery research. Especially, nanoparticles with specialized agents are used for cell-level detection, treatment and diagnoses of existing pathologies. Research activities in nano-medicine for treatment and diagnoses purposes rapidly become prevalent in the recent years since deaths by cancer cases are dramatically increased. According to World Cancer Report of The International Agency for Research on Cancer, the burden of cancer doubled globally between 1975 -2000 and it is claimed that it will double again by 2020 and nearly triple by 2030 (Boyle and Levin, 2008). Therefore, researchers tend to focus on medical diagnosis and treatment methodologies for cancer. Current medical methods of diagnosis and treatment for cancer have been changing and evolving by the impact of emerging technologies such as nanotechnology. Targeting delivery systems, diagnosis and imaging systems, regenerative medicine and tissue engineering are the most fundamental research and development areas related to both nanotechnology and biotechnology (Zhang et al. 2008).

Latest diagnostic imaging practices aim to develop nanoparticles which can carry specific contrast material so it would be targeted and directed from outside. Accordingly, it can be possible to obtain the detailed molecular imaging of the targeted tissues. The current research that focuses on targeted drug delivery combines NPs with the pharmacological agents. Nanoparticles are characterized according to the targeted tissues and used for treatments on the targeted tissue, even on one single cell. Therefore, understanding the NP-cell interactions is very important for targeted drug delivery and nanomedicine research. However, it is practically impossible to test all possible different combinations of NP characteristics to understand and generalize the effects of nano materials on biological systems. Consequently, this research aims to develop an ANN model that can realistically simulate the experimental results for any desired experimental setup without actually conducting the time-consuming and costly experiments.

In summary, the primary contribution of this study is to the area of nanomedicine by developing an ANN model for prediction of NP uptake rate. Furthermore, cellular uptake of NPs is simulated for multiple variations of NP characterization to understand NP-cell interactions instead of conducting thousands of experiments. The second major contribution is provided to the field of ANN by testing various feed forward multilayered ANN models with different training algorithms and different network structures. Specifically, this study demonstrates that optimal ANN model is achieved by using Bayesian regularization training algorithm with single hidden layer structure especially for small sized datasets.

The remainder of the thesis is organized as follows: A review of the relevant literature (e.g., ANNs modeling of NP-cell interactions and uptake of nanoparticles in cells) is given in Chapter 2. The experimental settings are discussed in Chapter 3. This is followed by the proposed ANN model in Chapter 4. Various ANN structures and optimization of several model parameters are discussed in Chapter 5. Finally the results of computational experiments are given in Chapter 6.

Chapter 2

Literature Review

In the literature there are many examples of different experimental studies related to cellular uptake rate of nanoparticles. In these studies nanoparticles that have different characteristics are being experimented to analyze the effects of NP features such as size, chemical structure, shape, surface charge and the concentration of NPs. In contrast, there are limited studies on mathematical modeling of NP-cell interactions.

Boso et al. (2011) conducted parallel plate flow chamber in vitro experiments to explore optimum nanoparticle diameter for which the number of adhering particles to diseased blood vessel walls is maximized. They use two different artificial neural network models with different internal structures which are trained with the flow chamber experiment data to the predict number of spherical nanoparticles adhering per unit area as a function of particle diameter and wall shear rate that depends to syringe pump flow rate. They found that an optimal particle diameter exists and artificial neural networks that demonstrate an accurate prediction can be used effectively to minimize the number of experiments needed. This study considers NP accumulation relations between only size and flow rate, but other properties of NPs such as type, shape, charge and concentration are not considered.

Rizkalla and Hildgen (2005) employed two commercial ANN models trained with 36 data to predict mean size and micropore surface area (MPSA) of polylactic acid (PLA) nanoparticles according to polymer concentration, pressure and polyvinyl alcohol (PVA) concentration which are emulsified in an organic phase with an aqueous solution of DNA. The results of Neuroshell1 Predictor (a black-box software adopting both neural and genetic strategies) and Neurosolutions1 (a step-by-step building of the network) were compared to those obtained by statistical method. It was concluded that NP size was influenced by PVA with large majority, but MPSA was influenced by the three variables, with the highest impact from polymer concentration. Moreover, predictions from ANNs were more accurate than non-linear regression results and output values which were closer to experimental values obtained by changing the network topology and parameters using Neurosolutions1. Even though this research is not directly related with cellular uptake of NP, it is significant with its solution method for mean size prediction of NPs.

Amani et al. (2008) perform 45 experiments to explore the effect of composition and processing factors on particle size of the nano-emulsion preparation for delivery of fluid drugs. The data from these experiments was applied to a commercial ANN model with 5 inputs variables: concentration of ethanol, budesonide, salinity, total energy and rate of applied energy. ANN model shows that the total amount of energy applied during nano-emulsion preparation was found to be the dominant factor in controlling the final particle size. This study does not discuss

cell interactions, but it provides knowledge about the nano-emulsion particles characterization and synthesis for drug delivery. Although they used ANN method, their specific problem is different from our study.

Lin et al. (2010) develop coarse-grained molecular dynamics (CGMD) simulation model for interactions between gold nanoparticles (AuNP) and cell membranes considering different signs and densities of surface charge on AuNPs. It is concluded that level of penetration increases as the charge density increases. Even though ANN is not used in this study, it helps to understand NP-cell interactions related to surface characteristics.

In the last decade NP-cell interactions was explored generally to understand the relationship of just two or three variables and ceteris paribus assumption holds which means that all the rest NP features and environmental specifications are kept the same. Asati et al. (2010) performed experiments to learn the cellular uptake and intracellular localization of the polymer-coated cerium oxide nanoparticles with respect to surface charges. NPs with positive, negative, and neutral surface charges were incubated with normal and cancer cell lines. They found that NPs with a positive or neutral charge enter both healthy and cancer cells, while NPs with a negative charge enter mostly in the cancer cells. In these experiments, time-dependent cellular uptake alteration was ignored and only the relation between cellular uptake and surface charge was investigated at the end of 3h incubation period. Peetla and Labhasetwar (2007) used polystyrene NPs of different surface charges and sizes to analyze changes in the membrane's surface pressure (SP).

Positive charged 60 nm NPs increased SP, neutral NPs reduced SP, and negative charged NPs of the same size had no effect. However, 20 nm NPs increased SP for all surface charge. Chithrani et al. (2006) investigated the impact of different size and shape of the gold nanoparticles over intracellular uptake inside mammalian cells. It was found that 50 nm gold nanoparticles reach cellular uptake at higher rates compared to smaller and larger sizes in the range of 10–100 nm. In another study, Davda and Labhasetwar (2001) observed that the cellular uptake of nanoparticles depends on the time of incubation and increased with increase in the concentration of nanoparticles in the medium. The overall conclusion is such that nanoparticle uptake into cells diverges as different sizes of NPs, different surface charges, different concentrations, different time points and different cell lines are preferred by different scientist. However, in all these existing studies NP-cell interactions are examined by only physical experimentations, without using a proper mathematical model. In this context, our study can be viewed as the first step towards mathematical modeling of these systems.

Although nano-medicine is a recent research area, applications of ANN in medicine cover a large variety of fields, including clinical diagnosis, image analysis and interpretation, signal analysis and interpretation and drug development (Sordo, 2002). ANN methodology mostly enhances the quality of the research. A systematic review which assesses the benefit of ANNs as decision making tools in the field of cancer shows that out of 396 studies involving the use of ANNs in cancer only 27 studies were either clinical trials or randomized controlled trials and out of these

trials, 21 showed an increase in benefit to healthcare provision and 6 did not (Lisboa and Taktak, 2005). Another review by Ahmed (2005) shows that applications of ANNs have improved the accuracy of colon cancer classification and survival prediction when compared to other statistical or clinicopathological methods. As a result, ANN appears to be a proper approach for modeling complex input-output relationships in medicine, as well as in nanomedicine.

Chapter 3

Basic Cell Structure and Particle Transportation

Organs are the collections of cells held together by intercellular supporting structures. There are 75-100 trillion cells in the body which are differentiated to perform special functions (Guyton and Hall, 2006). The function of each cell is coordinated by cells, tissues, organs or organ systems which consist of more than one regulatory system.

The basic function of all organs and tissues in the body is to keep the extracellular fluid level constant and balanced which is called "homeostasis". Human body has thousands of different control systems for the protection of the homeostasis. Cells in the body continue to live and function properly, as long as homeostasis is maintained. Each cell helps to protection of balance and benefit from homeostasis. Pathologies and diseases begin to emerge from the moment when this balance starts to deteriorate.

The cytoplasm which includes intracellular organelles (nucleus, endoplasmic reticulum, golgi apparatus, mitochondria, lysosome etc.) is separated from the extracellular fluid by the cell membrane. This membrane surrounding the cell is

composed from lipid bilayer with embedded proteins. This lipid bilayer is very high-permeable for fat-soluble substances such as oxygen, carbon dioxide and alcohol, but it forms a barrier against water-soluble substances such as ions and glucose. Proteins that have glycoprotein structure are floating in the lipid bilayer. Integral membrane proteins form structural channels (pores) which enables the transfer of the water-soluble substances, in particular ions from membrane. Carbohydrates located on the outer surface of cells membrane are mostly negatively charged and push away negatively charged substances that are close to the cell membrane.

There are many ways of particle transportation through the cell membrane. Basically, particles are transported via endocytosis, exocytosis, ion channels, diffusion or primary-secondary active transport methods (Guyton and Hall, 2006). Larger molecular structures (proteins) are taken into the cell via endocytosis. After protein connects to the membrane receptor, the cell membrane collapses inward. Contractile structures around indentation connect ends of membrane that surrounding the protein, thus a vesicle is generated within the cell. If there are protein, carbohydrate, fat and other basic structures of nutrients in vesicle, they are digested by lysosomal enzymes and converted to molecules such as amino acids, glucose and phosphate. These molecules are diffused to the cell cytoplasm. Vesicles that cannot be digested by lysosomal enzymes are called as residual body. They are disposed outside of the cell by a reverse endocytosis mechanism called exocytosis. Cell membrane lost during endocytosis is re-earned by exocytosis so that the membrane integrity is preserved. Active transport is defined as the material transport through

membrane with the help of a carrier against an electrochemical gradient. Therefore, an additional energy source is required. Diffusion is the transport of material from where electrochemical and concentration of the material is very intense to less dense by its own kinetic dynamics without requiring an additional energy. This form of transportation, molecules or materials is transmitted through either gaps between the lipid bilayer (simple diffusion) or carrier proteins (facilitated diffusion / carrier-mediated diffusion).

There are various factors that influence transport of particle through the cell membrane from one side to the other side. These are:

- Membrane Permeability: Permeability of different cell membranes is varied for different particles. Permeability of a membrane for a particle is the speed of propagation on the unit area of membrane caused by the concentration difference between both sides of the membrane (without electrical difference or pressure difference).
- Concentration Difference: A particle's net speed of propagation on cell membrane is directly proportional to the concentration difference on both sides of the membrane.
- Electrical potential difference: Cells allow the transfer of charged ions if difference of electrical charge between two sides of the membrane is constant. However, if this electrical balance is disturbed and the concentration of particles in any charge (within or outside the cell) increases, the transportation of the charged particles that have more density will increase. Since the transportation

resulting from the concentration difference begin to increase the electrical potential difference after a period of time, the transportation will stop over time and will reach the balance.

- Other: In addition to the above, shape, size and chemical structure of the macro-molecules is very effective on transportation through the cell membrane. It is easier to transport macro-molecules that are nanometer-sized, smooth-rounded shaped and have bio-compatible chemical composition.

Chapter 4

Experimental Procedure of Proposed Study

Synthesis of nanoparticles used for targeted drug delivery and detection of existing pathologies at cell-level require special expertise and advanced technology applications. These synthesized NPs should be characterized according to targeted cell/tissue in order to find and adhere to the target cell/tissue in chaotic environment of the organism. Therapeutic (curative) agents are placed inside or on the surface of the chemically or immunologically characterized NP for the purpose of treatment. Furthermore it is possible to place both therapeutic and diagnostic contrast agents together. This new method allowing simultaneous cell-level treatment (therapy) and diagnosis is called "theragnostic". NPs that are used for theragnostic purposes have five key variables: size, chemical structure (type), shape, surface charge and the concentration of NPs (NP amount /ml^3).

The data set for the ANN model is provided through in-vitro nanoparticle-cell interaction experiments conducted by Hacettepe University, Department of Nanotechnology and Nanomedicine. Considering scientific constraints and priorities, three different types of NPs were prepared for in-vitro nanoparticles - healthy cell interaction experiments: polymethyl methacrylate (PMMA), silica and polylactic

acid (PLA). These NPs are all sphere-shaped. Two different diameter sizes of NPs (50 nm and 100 nm) are preferred for PMMA and silica nanoparticles, and only one diameter size of NPs (150 nm) is preferred for PLA; two different surface charge (positive and negative) were formed for each type of NPs. Certain concentrations of NPs (0,001 mg/l and 0,01 mg/l) were interacted with healthy cells. Cellular uptake rate of NPs was measured at specific time intervals. Transmission electron microscopy (TEM) is used to determine the size and size distribution of NPs inside and over the surface of the cells and surface charges were determined by zeta potential measurements.

Nanoparticles were subjected to interact with cells in vitro by using micromanipulation systems in the labs established as a "clean room" principle. Spectrophotometric measurement methods, transmission electron microscopy and confocal microscopy were applied in order to observe NP-cell interactions and to get the data. For this experiment, "3T3 Swiss albino Mouse Fibroblast" type of healthy cell set was used. Cells were incubated in medium containing 10% FBS, 2 mm L-glutamine, 100 IU / ml penicillin and 100 mg / ml streptomycin at 37 °C with 5% CO2. After incubation, proliferating cells in the culture flask were passaged using PBS and trypsin-EDTA solution. Then, cells incubated for 24 hours were counted and placed on 96-well cell culture plates. Next, previously prepared solutions containing specific concentrations of nanoparticles were added to those plates.

Experiments were repeated six times for each of the 20 different configurations of nanoparticles. In order to determine variation of NP-cell interaction by time, cell

cultures were observed at 3, 6, 12, 24, 36 and 48 hours of incubation. At the end of the incubation period, the number of NP removed from the environment is determined with washing solution. By subtracting this value from the initially applied total number of NPs, the number of NPs attached to the cell surface or the number of NPs entered into the cell was determined. Then, cellular uptake efficiency of nanoparticles is calculated by dividing the number of NPs over the cell surface and inside the cell to the total number of applied NPs.

Chapter 5

A Brief Description of ANNs

Artificial neural networks are inspired by the systems of nerve cells in the brain. ANNs accurately estimate nonlinear relationships between inputs and outputs by imitating the complex processes of the brain. Although brain activities are tremendously complicated, modeling of a nerve cell known as neuron gives detailed information about biochemical reactions. ANNs provide sufficient structure for the neural system to understand biological processing of neurons. This structure has huge numbers of processing units and interconnections between them. Each unit or node is a simplified model of a biological neuron which receives input signal from the previous linked neurons and sends off output signals to subsequent linked neurons.

The general mathematical description of a neuron is defined as follows:

$$y(x) = f\left(\sum_{i=0}^{n} w_i x_i\right)$$

x is a neuron with n input dendrites $(x_0 , \dots , x_n)$ and one output axon *y(x)* and where $(w_0 , \dots , w_n)$ are weights defining how much the inputs should be weighted.

The simple processing unit of neural network is shown in Figure 1. On the left side inputs are connected to neuron j and each connection has an associated weight given as w_{ij}. Neuron j computes its output by performing a differentiable transfer function 'f' on weighted sum of inputs plus a bias term 'b'. The bias term allows us to compensate errors for the data. This output value is sent along all the output connections shown at the right.

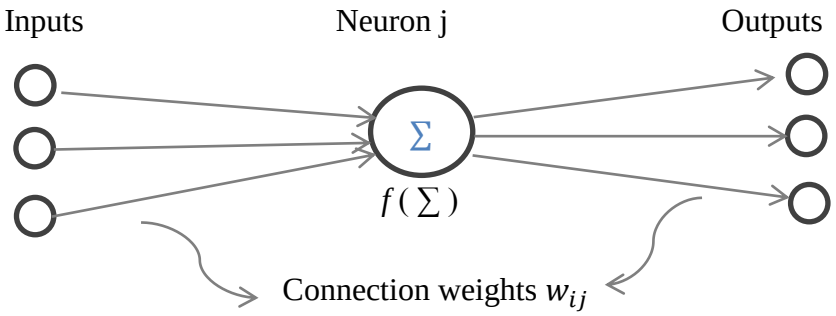

Figure 1. Neuron model

Neurons form a multilayered structure by connecting each other. The basic multilayered network consists of three layers described as input layer, hidden layer and output layer. There is a full connection between nodes of each layer. Since the data flow has one direction through input layer neurons to output layer neurons, the network is called as feed-forward network. Multilayered structure permits more than one hidden layer. It is possible to make the network more flexible and accurate by increasing both the number of hidden layers and hidden neurons on those layers. However, the computations take more time and more resource as the number of

hidden layers and neurons are increased (Aizenberg, 2006). Furthermore, increasing the number of hidden neurons causes over-fitting problem.

Nonlinear relationships between input and output values are predicted by the multiple layers of neurons with nonlinear transfer functions. The linear transfer function for output vector is frequently used in function fitting or nonlinear regression problems.

Three-layer network of the ANN algorithm on Neural Network Toolbox - User's Guide (Beale, 2011) is depicted in Figure 2 using shortened notation:

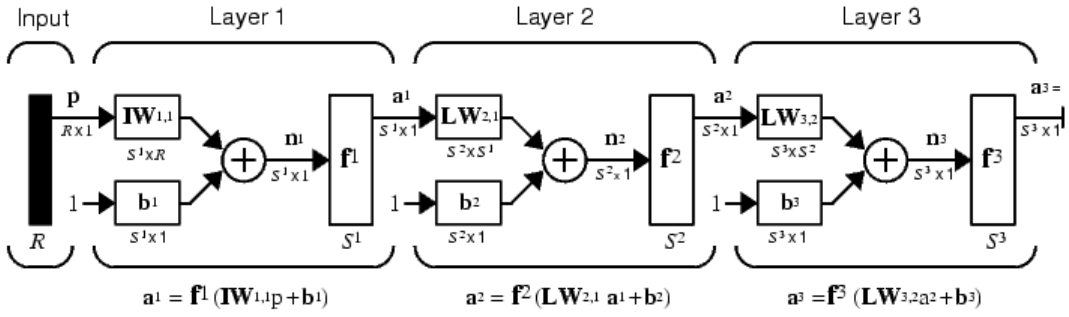

$$Output = a^3 = f^3\,(LW^{3,2} f^2\,(IW^{2,1} f^1\,(IW^{1,1} p + b^1) + b^2) + b^3) = y$$

Figure 2. Three-layered ANN model

This network has an input vector 'p' consisting of R neurons, 2 hidden layers with S^1 and S^2 neurons respectively and an output layer with S^3 neurons. A bias term *'b'* is added to input weight (*IW*) matrices as well as layer weight (*LW*) matrices as a single neuron. Output of the multilayer network 'y' is equal to output of last layer *'a^3'*. Neurons generate their output 'a' by using differentiable transfer functions *'f'*.

Training is supervised when the output values are introduced with the corresponding input pattern. On the other hand, unsupervised networks adjust weights according to the similarity of the inputs without presenting output values. Since prediction of output is the objective of our model, we utilize from supervised training.

The weights for each interconnection are regulated during the training to create the ultimate ANN. The training procedure can be seen as an optimization problem, where the objective is to minimize mean square error (MSE), mean absolute error (MAE) or sum squared error (SSE). The general performance function for feed-forward networks is MSE, which is the average squared error between the predicted output values *'a'* and the actual outputs *'t'*.

MSE is stated in equation below:

$$MSE = 1/N \sum_{i=1}^{n} e_i^2 = 1/N \sum_{i=1}^{n} (t_i - a_i)^2$$

The most widely used ANN learning method is a specialized gradient descent algorithm called as Back Propagation (BP) Learning Algorithm (Rumelhart et al. 1986). BP learning algorithm adjusts the weights depending on the error between actual output value and predicted output value of the ANN. BP method first propagates an input through the network to the output and calculates the error. Then the error is propagated backwards over the network while the weights are changed in order to minimize the error. Lowery et al. (2009) shows back propagation of weights as it is seen on Figure 3. After the weights are changed, the hidden layer neurons are

generated their outputs and the error is determined again. If the iteration number has not reached its limit, the error will be back propagated to the input layer once more. This training process continues until a certain stopping criterion is reached. The stopping criteria can be minimum gradient magnitude, maximum number of validation increases, maximum training time, minimum performance value, maximum number of training epochs (iterations). When one of these values reaches a definite limit, the training is stopped.

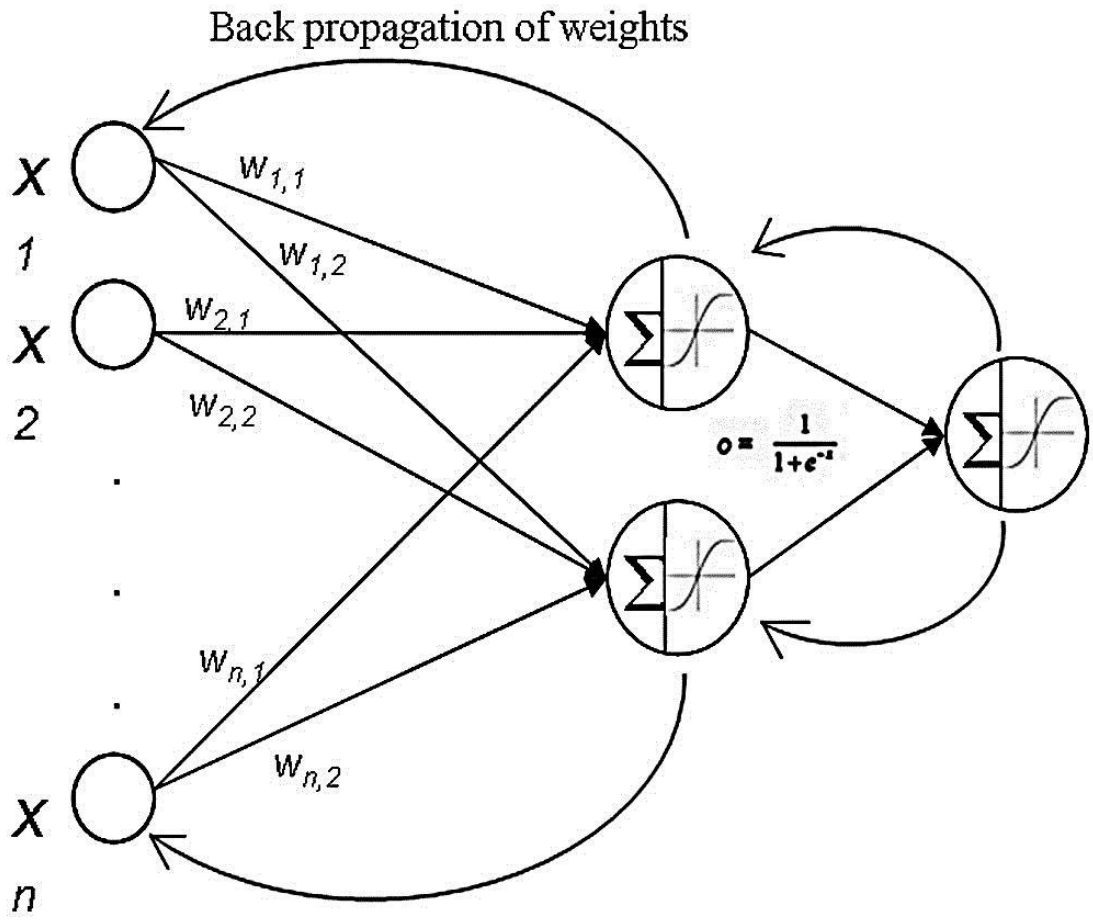

Figure 3. Back Propagation learning scheme

Chapter 6

The Proposed ANN Structure

The proposed model is implemented on MATLAB Programming Language. It is a multilayer feed forward network and the training process is performed with the back propagation algorithm. As seen in Figure 4, the network consists of input layer with 5 nodes, one hidden layer with n nodes and one output layer with one node. There are many-to-many feed forward connections between input nodes and hidden nodes, whereas many-to-one feed forward connections between hidden nodes and output node.

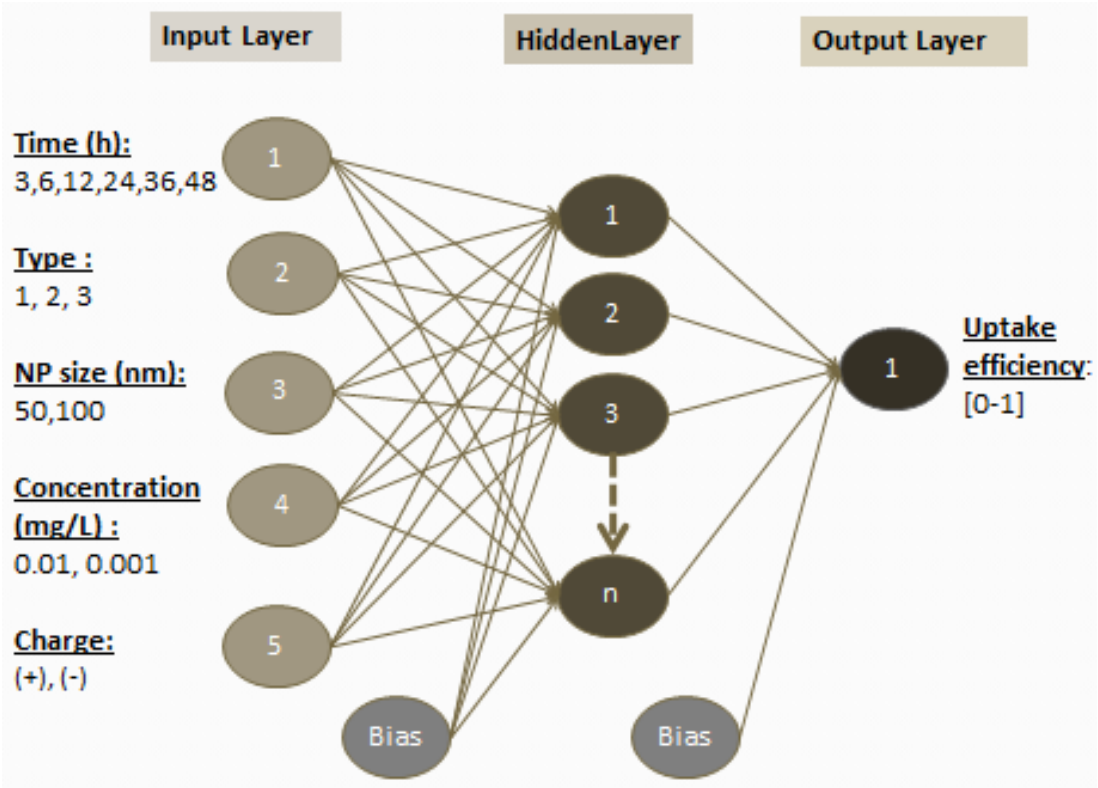

Figure 4. ANN architecture

The data set for the ANN model is obtained from in-vitro nanoparticles-cell interaction experiments. The current values of the input variables are given in Table 1. Type and charge of NPs are categorical variables, whereas size, concentration and incubation time are numerical variables. Categorical variables should be converted to numerical values in order to be modeled mathematically. Numerical values for type and charge is written next to them in parenthesis below. Performing preprocessing steps such as normalization on the network data increases the efficiency of ANN training. Therefore, normalization of inputs to fall in the range [-1, 1] is performed, after all inputs are represented as numerical variables.

Table 1. Input variables

Input neuron	**Value**
Types of NPs	PMMA (1), Silica (2), PLA (3)
Diameter size of NPs	50 nm and 100 nm for PMMA and Silica 150 nm for PLA
Surface charge of NPs	Positive (+1) and Negative (-1)
Concentrations of NPs	0,001 - 0,01 mg/l
Incubation time	0,3, 6, 12, 24, 36, 48 hours for PMMA, Silica and PLA 0,1.5, 4, 9, 18, 30, 42 hours for silica

Output of the proposed ANN model is cellular uptake efficiency of NPs which is the one and only dependent variable of the experiments. Therefore, output layer has one neuron that represents uptake efficiency. Uptake efficiency is a ratio of NPs

over the cell surface and inside the cell to the total number of applied NPs (in the range [0, 1]).

In general, either hyperbolic tangent sigmoid transfer function (tansig) is used for hidden layers to generate outputs between -1 and 1 or logarithmic sigmoid transfer function (logsig) is used to generate outputs between 0 and 1. We preferred tansig transfer function for the hidden layers because of the fact that outputs of all hidden neurons are between -1 and 1. Moreover it is confirmed that two-layer tansig/purelin network can properly approximate any function with sufficient neurons in the hidden layer (Beale, 2011). Since the output value is a rate between 0 and 1, it is better to use saturated linear transfer function (satlin) instead of linear transfer function (purelin) for output layer. Consequently, it is ensured that output value falls in the range [0, 1]. Graphics of tansig and satlin transfer functions are displayed in Figure 5 and Figure 6, respectively (Beale, 2011). Tan-Sigmoid Transfer and Saturated Linear Transfer functions are given by

$$f(x) = \frac{2}{1+e^{-2x}} - 1 \text{ and } f(x) = \begin{Bmatrix} 0, & if\ x < 0 \\ x, & if\ 0 \le x < 1 \\ 1 & x \ge 1 \end{Bmatrix}, \text{ respectively.}$$

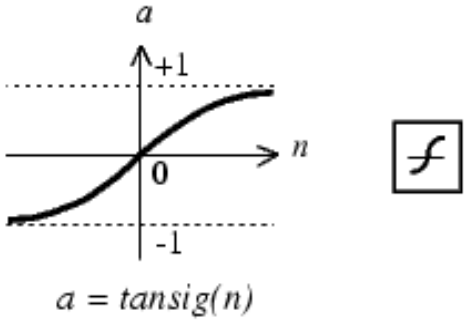

Figure 5. Graphic of tan-sigmoid transfer function

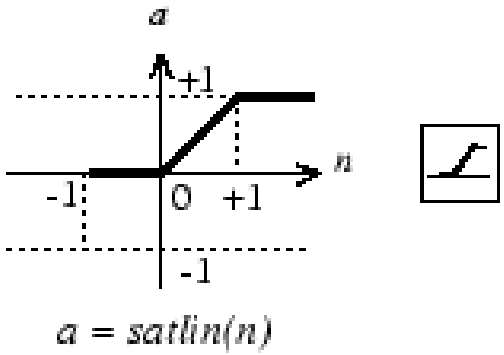

Figure 6. Graphic of saturated linear transfer function

The dataset that comes from the nanoparticles-cell interaction experiments is divided randomly into training and test dataset. The training dataset is used for fitting the neural networks model. Test dataset is used after the training for the evaluation of performance of the model output. An unbiased estimation of the generalization error of the model is provided by the error on the test dataset. This simple validation method is known as test set validation.

Data allocation for training dataset and test dataset is very important, since our experimental dataset is small. Each different combination of input variables forms 20 different classes and 6 experiments was conducted for each class. Numbers of samples are 672, 336 and 168 for silica, PMMA and PLA, respectively. Increasing the class imbalance in the training dataset generally gives a gradually unfavorable result on the test performance for small and moderate size training datasets that contain either uncorrelated or correlated features (Mazurowski et al., 2007). Therefore, randomly selected one sample is used for the test dataset, and remaining five samples is used for the training dataset for each different combination of input

variables. This method is called split-sample cross validation. In this manner, 196 samples are allocated for test from total of 1176 samples.

For each run of the algorithm MATLAB starts from different random seed and hence generates different solutions depending on randomized weight adjustments. To be able to measure the effect of the different parameter values in the same experiment, we initialize the seed to a fixed value.

6.1 Training Parameters

MSE is used as the network performance function during the training process. In general there are two training schemes: Batch training and incremental training. In the former case, weights and biases are adjusted after all inputs and outputs are presented to the network completely. In the latter case, however, weights and biases are adjusted after each input is presented to the network one by one. Batch training is preferred for this ANN model since it is better than incremental training by means of fastness and error minimization.

Several variations of BP methods exist in the neural network toolbox of MATLAB under the title of training function algorithms (see Table 2). The performances of all 14 different training functions are measured in terms of MSE and execution time (note that each training function has different parameters according to their weight adjustment techniques).

Table 2. BP training functions

Function	**Algorithm**	**# Parameters**
Trainb	Batch training with weight and bias learning rules	4
Trainbfg	BFGS Quasi-Newton	17
Trainbr	Bayesian Regularization	10
Traincgb	Conjugate Gradient with Powell/Beale Restarts	16
Traincgf	Fletcher-Powell Conjugate Gradient	16
Traincgp	Polak-Ribiére Conjugate Gradient	16
Traingd	Gradient Descent	7
Traingda	Gradient descent with adaptive learning rate	9
Traingdm	Gradient Descent with Momentum	7
Traingdx	Variable Learning Rate Gradient Descent	10
Trainlm	Levenberg-Marquardt	10
Trainoss	One Step Secant	16
Trainrp	Resilient Backpropagation	10
Trainscg	Scaled Conjugate Gradient	7

Although number of parameters for each training functions are different, some of the parameters are common for all training functions. The default parameter values are selected for distinct parameters and only the common parameters are

changed to achieve better performance for all training functions. After several executions of training algorithms, the final parameter values are set in Table 3.

Table 3. Common parameters of the training functions

Parameter	**Default Value**	**Post-defined Value**
Maximum number of epochs to train	100	2000
Performance goal	0	0
Maximum time to train in seconds	inf	inf
Maximum validation failures	5	10
Minimum performance gradient	1.00E-10	1.00E-10

Performance of training functions are tested with 3 different layer structure: [5-5-1], [5-10-1], [5-15-1]. The first number is input node number, second number is the nodes in hidden layer (HL) and last number is the output of the network. Comparison of training performances is shown in Table 4. According to these performances, the best training function among overall functions is Bayesian regularization (*trainbr*) in terms of both minimum MSE over test dataset and minimum elapsed time. *Trainbr* adjusts the weight and bias values according to Levenberg-Marquardt optimization method. During the Bayesian regularization process, a combination of squared errors and weights are minimized in order to find the best combination, which indicates that its generalization capability is fairly high. As can be seen in Table 4, Levenberg-Marquardt (*trainlm*) also yields promising results even though it not as good as *trainbr*.

Table 4. Performance of training functions

	# Node in HL=5		# Node in HL=10		# Node in HL=15	
Training Function	**MSE**	**Elapsed Time (sec)**	**MSE**	**Elapsed Time (sec)**	**MSE**	**Elapsed Time (sec)**
'trainbr'	0.0083	5.02	0.0031	12.45	0.0018	20.87
'trainlm'	0.0103	41.11	0.0037	52.07	0.0029	63.43
'traincgb'	0.0104	23.12	0.0040	53.51	0.0040	57.11
'trainbfg'	0.0105	9.69	0.0056	34.51	0.0042	69.31
'traincgp'	0.0110	23.13	0.0043	52.56	0.0035	57.25
'trainoss'	0.0112	19.83	0.0054	47.44	0.0071	50.23
'trainrp'	0.0136	10.37	0.0087	24.88	0.0064	26.68
'traingdx'	0.0160	9.22	0.0185	20.09	0.0217	22.99
'trainscg'	0.0188	19.14	0.0045	47.24	0.0038	53.43
'traincgf'	0.0223	9.89	0.0051	52.67	0.0030	56.94
'traingda'	0.0447	9.33	0.0343	21.08	0.0360	23.96
'trainb'	0.0661	8.92	0.0517	19.94	0.0501	23.18
'traingdm'	0.0812	9.16	0.0685	21.22	0.0547	23.54
'traingd'	0.0812	8.83	0.0687	21.90	0.0548	23.82

6.2 Number of Hidden Layer and Neurons

It is argued that the best number of hidden neurons depends on too many variables such as the numbers of input and output units, the complexity of the problem, the number of training iterations, the amount of noise on the data, the architecture of the network, the training algorithm (Xu and Chen, 2008). Quite a few researches propose different rules for deciding on an optimal number of hidden neurons. However, these rules are generally problem specific and ignores some related variables stated above. Therefore, we should need to decide a method for optimal number of hidden neurons which is special to our problem. In order to find best network structure, the number of hidden layers and the number of neurons on them obtained by trial and error method.

Feed-forward networks can learn complex relationships more quickly if the network has more than one hidden layer. However, Haykin (1999) proposes that at most two hidden layers are sufficient to model every ANN problem. In our study we tested both one and two hidden layers with different number of nodes. As seen in Figure 7, first hidden layer nodes from 1 to 20 and second layer hidden nodes from 0 to 20 are combined and in total 420 different ANN structures are tested. MSE values for single hidden layer with neurons from 1 to 20 are presented in the graph with zero number of nodes in the second hidden layer. Minimum MSE is equal to 0.0012 and it is achieved with the structures which have more than 18 neurons in sum of 2 hidden layers. Accordingly, the performance achieved by two hidden layer is

comparable with one hidden layer that has more than 18 neurons. It is advantageous to use single hidden layer since an increase on the number of hidden layers extends the computation time. For this reason, a single hidden layer ANN structure is used in our study.

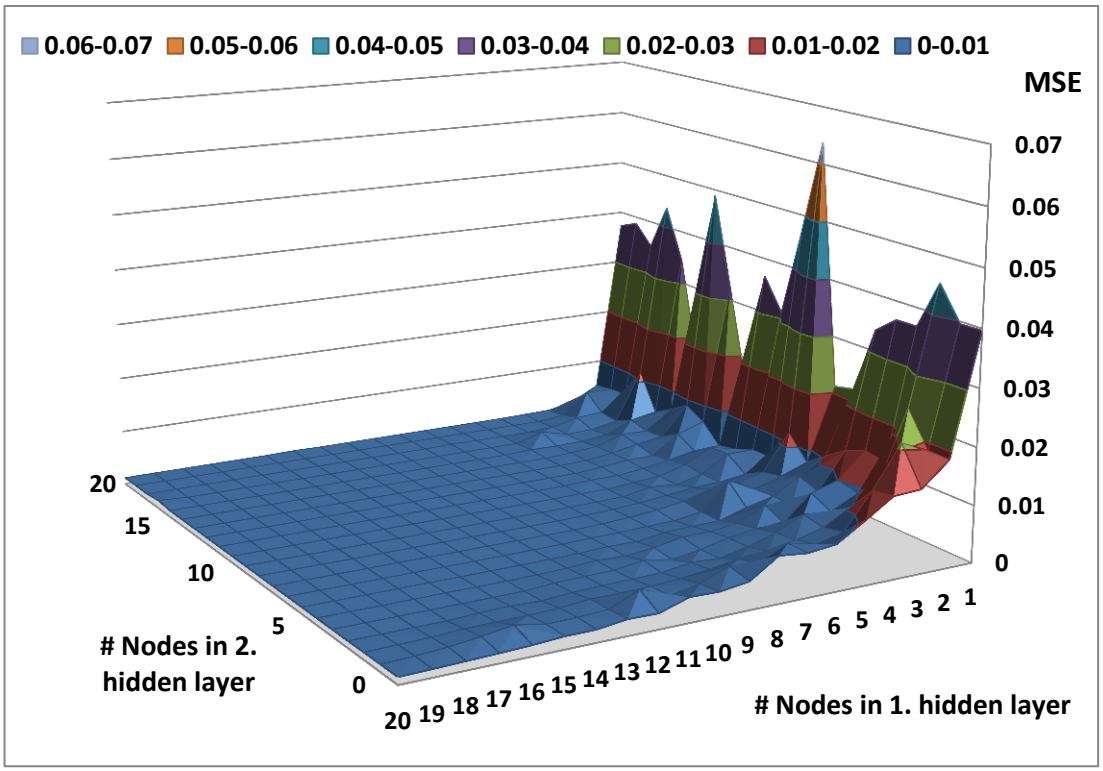

Figure 7. MSE of 2 layer ANN models

Adding extra nodes to hidden layer contributes to build more advanced ANN model. However, too many nodes on the hidden layer decrease the error on training dataset, while the error on test dataset becomes large. In other words, network memorizes the training pattern instead of learning. It cannot make good generalizations when the network encounters a new input sample. On the other hand, too few hidden nodes cause under-fitting due to high bias values and give high

training errors. As in the case of excessive nodes, insufficient nodes also show poor generalization ability. In order to avoid over-fitting and under-fitting, it is required to find best node number by trial and error method. Henceforward, the impact of number of neurons in the hidden layer on performance functions is analyzed from 1 to 20 nodes.

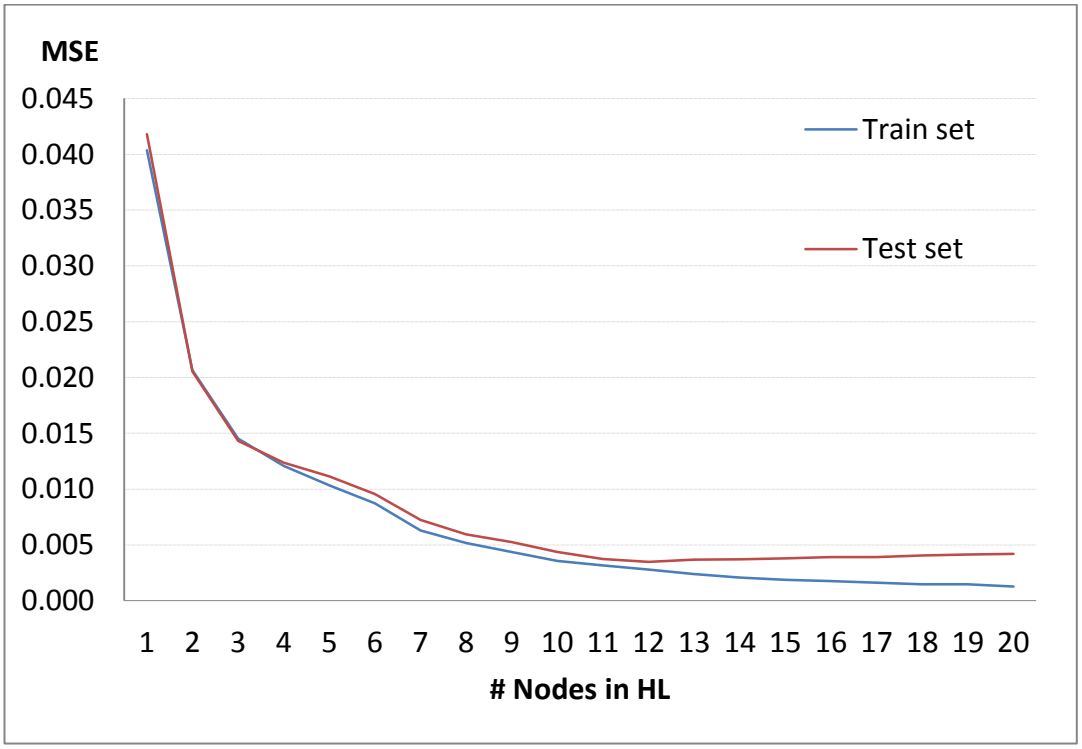

Figure 8. MSE of one layer ANN models

Figure 8 shows the MSE of the networks that have different node numbers. According to these results, increasing the numbers of nodes leads to exponential decay in the MSE. It is seen that up to 5 nodes under-fitting arises, since MSE values are very large (more than 0,01). After 8 nodes, an increase on the number of nodes affects MSE less than 1/1000. Still, MSE value for the train set continues to rise slightly up to 20 nodes. On the contrary, after 12 nodes MSE values for the test set

increase a little. In other words, over-fitting occurs when more than 12 nodes are used in the hidden layer. According to trial and error method, best number of nodes in the hidden layer is 12.

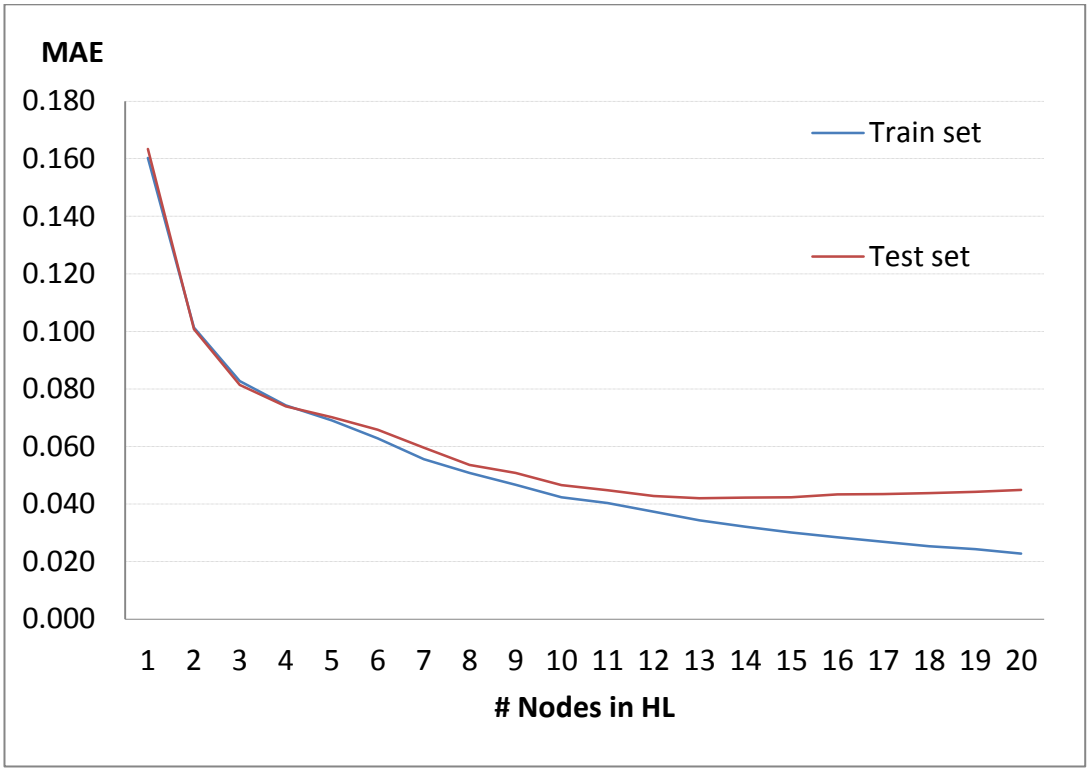

Figure 9. MAE of one layer ANN models

MAE of the networks is analyzed in Figure 9. Similar to MSE, MAE values also decay exponentially as the node numbers increases. However, the difference between training set and test set is seen more explicitly. It is distinguished that over-fitting with more than 12 nodes and under-fitting with less than 5 nodes are occurred as well.

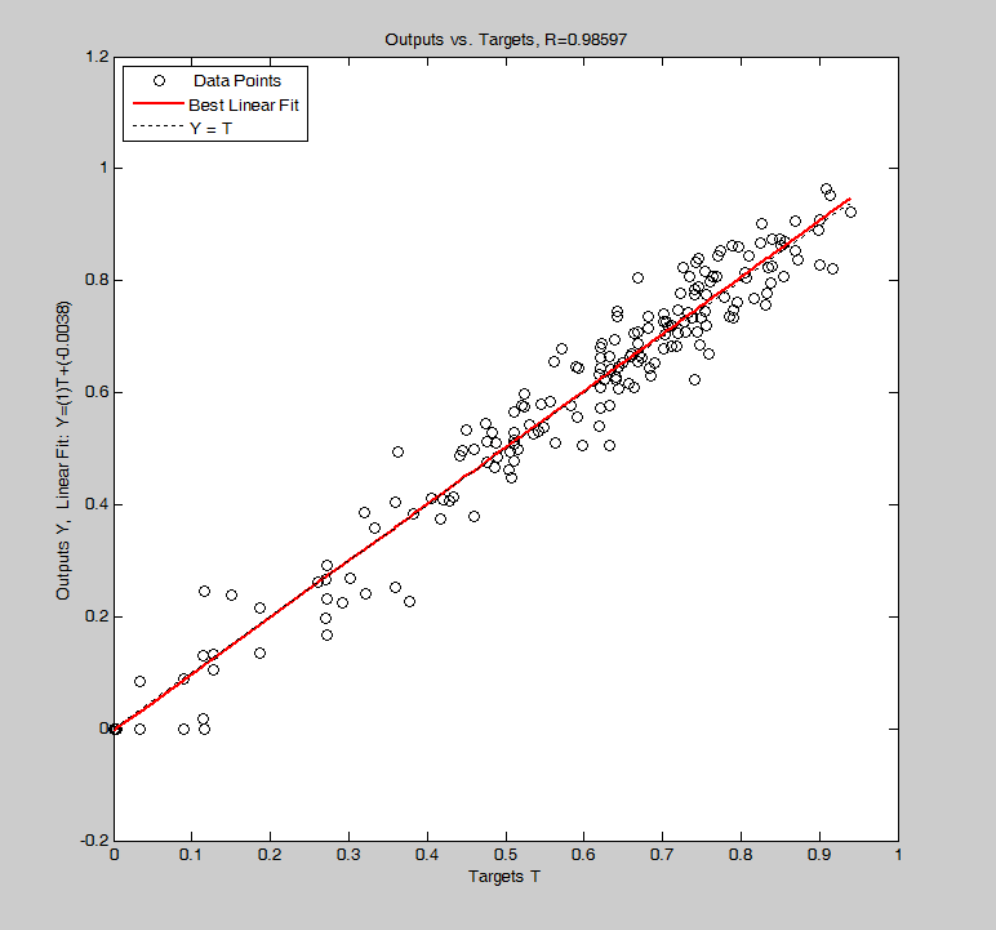

Figure 10. Linear fit of test data

The regression result of the test data is shown in Figure 10. The solid red line represents the best fit linear regression line between predicted outputs and actual targets. The relationship between the outputs and targets is indicated with the R value. There is a perfect linear relationship between outputs and targets, if R value equals to 1. There is no linear relationship between outputs and targets, if R is close to zero. The test data points show good fits with R=0.9859. Since training data and test data division is very balanced, there is no extrapolation. In other words, all data points in test set are inside of the range of the training set.

Chapter 7

Simulation Results

NP uptake rate is simulated for 48-hours via optimized ANN model. The proposed ANN model has 5-12-1 network structure and implements Bayesian regularization training algorithm. Predicted values of NP uptake rate are shown in 20 different charts for each different class that varied according to the characteristics of NPs. Simulation runs are repeated 50 times for all different types of NP-cell interactions. For each of 50 different simulation runs, different initial parameters are set and the best of them are chosen as the final fit of the model. Mean values of these 50 predicted samples are plotted as black line in the charts below. Confidence bounds which are plotted with blue dotted line are calculated with $\pm 2\sigma$ standard deviations of the predicted 50 samples for each hour from 1 to 48. Moreover, actual data obtained from experiments are plotted with red x-mark.

As seen from the charts, confidence intervals change at each hour. Standard deviations are small at the hours where actual data is known. However, standard deviations are large at the hours where actual data is not observed. Actual data stay within the confidence interval for PLA, and too few ones are out of the confidence bounds for PMMA and Silica.

Simulation results are given in Figure 11-16. After adding nanoparticles on cell lines, a fast cell adhesion and entry process is realized in the first 3-hour. Although the overall behavior of NP uptake varies according to NP characteristics, the general behaviors are similar in all the figures. At the beginning of the incubation period, there is a rapid entry of NPs into the cell. After a while, there is a reduction in NP uptake rate and then again it increases and continues to fluctuate in this way. In order to make more accurate generalizations, each NP type should be evaluated separately.

The simulation results of the uptake rates of PMMA nanoparticles are displayed in Figure 11 and Figure 12. Standard deviation of mean uptake rates of hours is given in table below. When size and concentration are constant, negative charged NPs have smaller standard deviations. This proves that positive charged NPs show large fluctuations than negative charged NPs for PMMA. When negatively charged PMMA NPs are compared in terms of concentration with constant NP size, high concentration (1/100) has smaller standard deviations; so it gives more stable uptake rate results than low concentration (1/1000).

Table 5. Standard deviation of mean uptake rates for PMMA

Type	PMMA							
Size	50				100			
Charge	-1		1		-1		1	
Concentration	0.001	0.01	0.001	0.01	0.001	0.01	0.001	0.01
Average of mean uptake rates	0.509	0.506	0.340	0.549	0.537	0.260	0.265	0.539
Standard deviation of mean uptake rates	0.142	0.098	0.167	0.156	0.133	0.060	0.280	0.230

Hypothesis testing for the difference between two means is applied to understand the effect of 50 and 100 nm sizes for negatively charged PMMA. For each hour from 1 to 48, mean and standard deviations of 50 samples are calculated. The central limit theorem states that the sampling distribution of a statistic will be approximately normal if the sample size is greater than 40. Thus, each sample is independent simple random sampling with approximately normal distribution. Two-sample t-test is appropriate to determine whether the difference between means found in the sample is significantly different from the hypothesized difference between means.

Null hypothesis: effects of 50 and 100 nm sizes are the same

Alternative hypothesis: effects of 50 and 100 nm sizes are different

When the null hypothesis states that there is no difference between the two population means, the null and alternative hypothesis are stated as H_0: $\mu_1 = \mu_2$ and H_a: $\mu_1 \neq \mu_2$ respectively.

Significance level is 0.05 for this analysis. The degrees of freedom (DF) is n-1=49.

Standard error is computed as $SE = \sqrt[2]{(\sigma_1^2/n_1)+(\sigma_2^2/n_2)}$ and t-score test statistic $t = \frac{[(\mu_1-\mu_2)-d]}{SE}$ where μ_1 is the mean of sample 1, μ_2 is the mean of sample 2, d is the hypothesized difference between population means (d=0 for this case), σ_1 is the standard deviation of sample 1, σ_2 is the standard deviation of sample 2, and $n_1$is the size of sample 1, and $n_2$is the size of sample 2.

The null hypothesis is rejected when the P-value is less than the significance level. We have a two-tailed test; P(t < -2.01) = 0.025 and P(t >2.01) = 0.025. In order to

have P-value is less than the significance level (0.05), t-score should be less than -2.01 or greater than 2.01. In other words, we fail to reject null hypothesis if t-score is between -2.01 and 2.01.

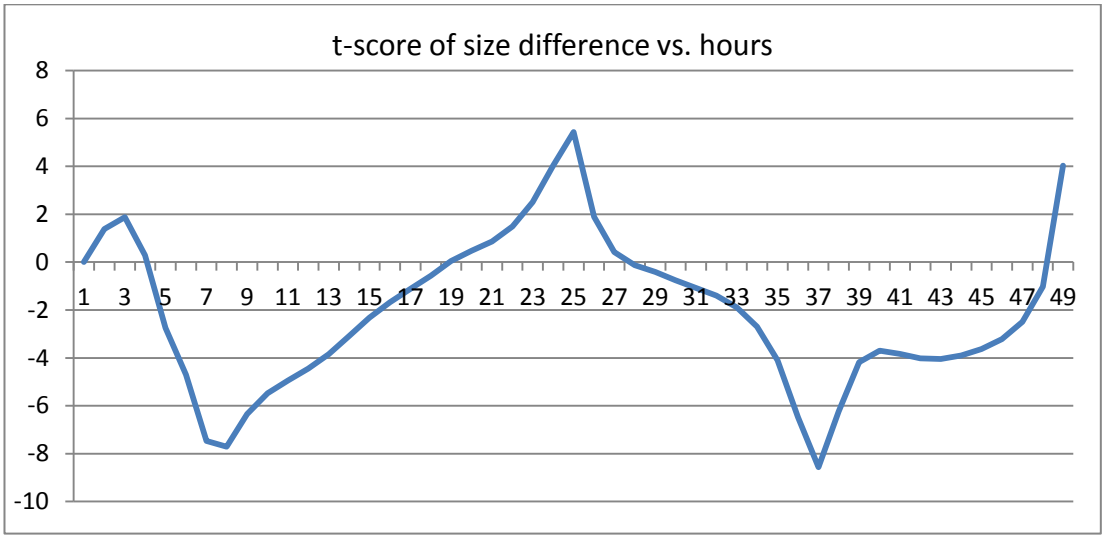

Figure 11. t-score of size difference ((-) Charged PMMA NPs, 0.001 Concentration)

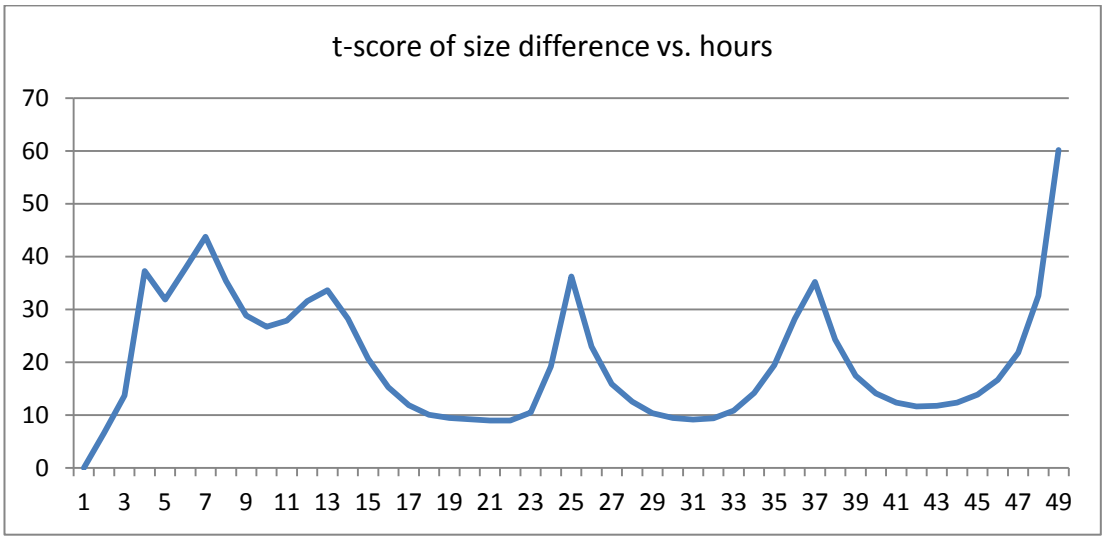

Figure 12. t-score of size difference ((-) Charged PMMA NPs, 0.01 Concentration)

In (-) charged low concentration case, P-value is sometimes less than the significance level sometimes not. There is no clear difference between 50 nm and 100 nm sizes. It is also seen from simulation results that there are not very meaningful differences between 50 and 100 nm dimensions. In (-) charged high concentration case, the null hypothesis is rejected since t-scores are always more than 2.01; this shows 50 nm size lead to high uptake rate. According to results, it is more appropriate to prefer (-) charged, 50 nm and high concentration of NPs for more stable and high uptake rate results in a targeted distribution system with PMMA type of NPs.

The simulation results of the uptake rates of Silica NPs are given Figure 13 and 14. Two-sample t-test, which has same procedure as described above for PMMA, is conducted for difference of 50 and 100 nm sizes of silica NPs. For (-) charged NPs, the null hypothesis is rejected since t-scores are always less than -2.01; this means that 100 nm size lead to high uptake rate. However, there is no clear difference between the effect of 50 or 100 nm sizes for (+) charged NPs in 0.001 concentration, because null test is rejected for some hours and failed to reject for the other hours. For (+) charged NPs in 0.01 concentration, t-scores are always more than 2.01; this means that 50 nm size lead to high uptake rate.

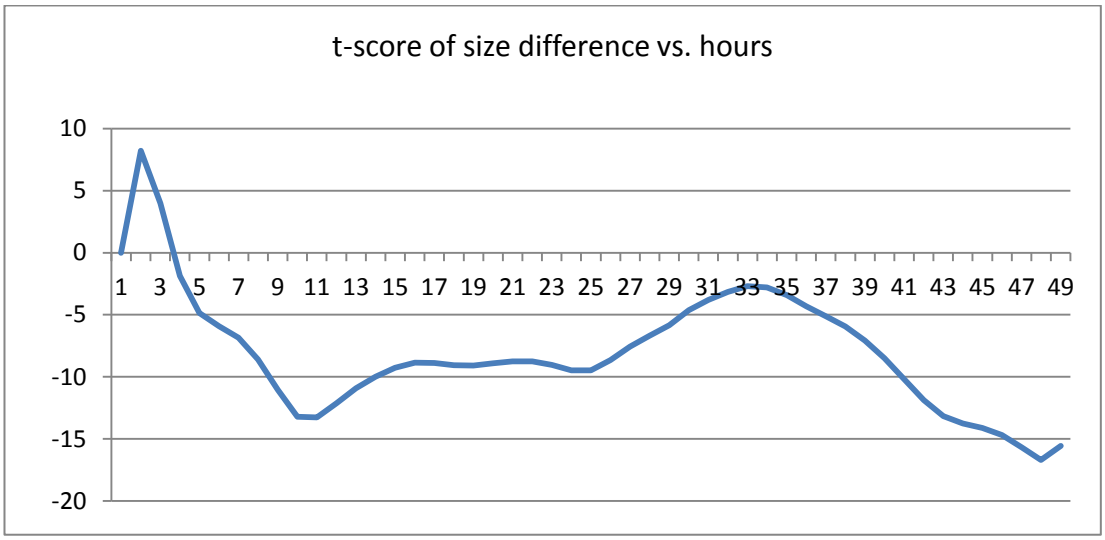

Figure 13. t-score of size difference ((-) Charged Silica NPs, 0.001 Concentration)

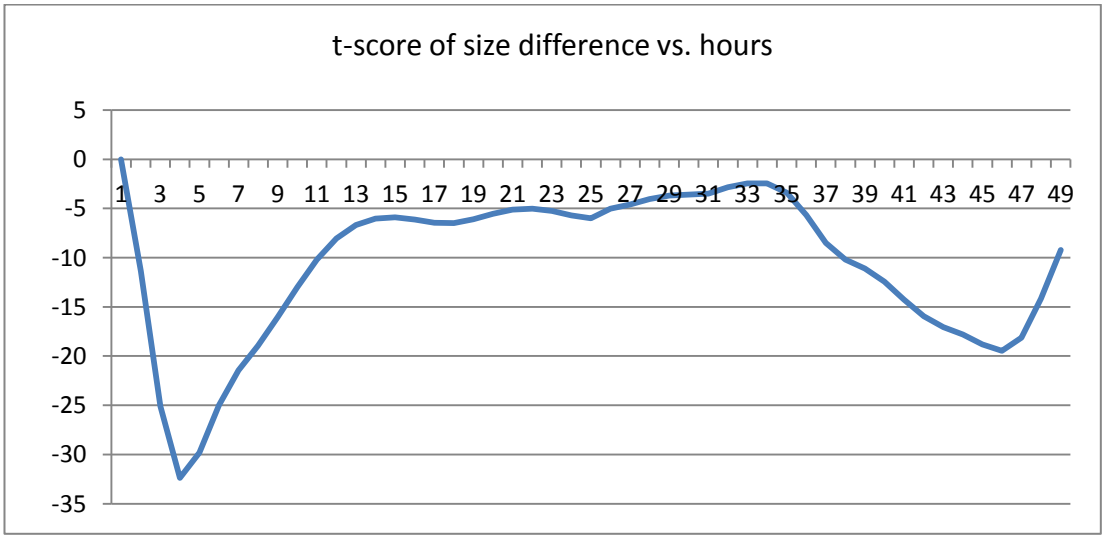

Figure 14. t-score of size difference ((-) Charged Silica NPs, 0.01 Concentration)

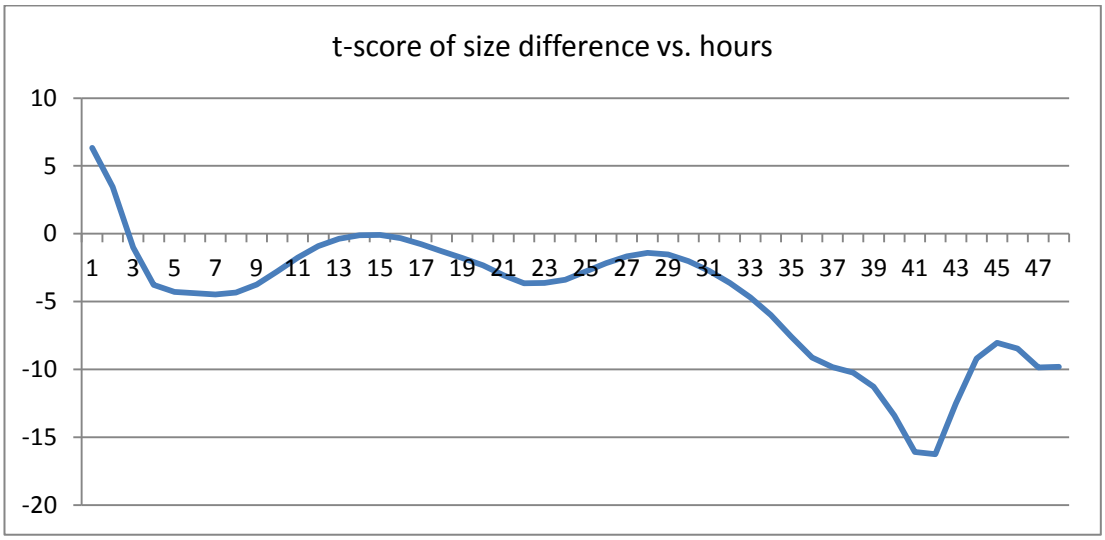

Figure 15. t-score of size difference ((+) Charged Silica NPs, 0.001 Concentration)

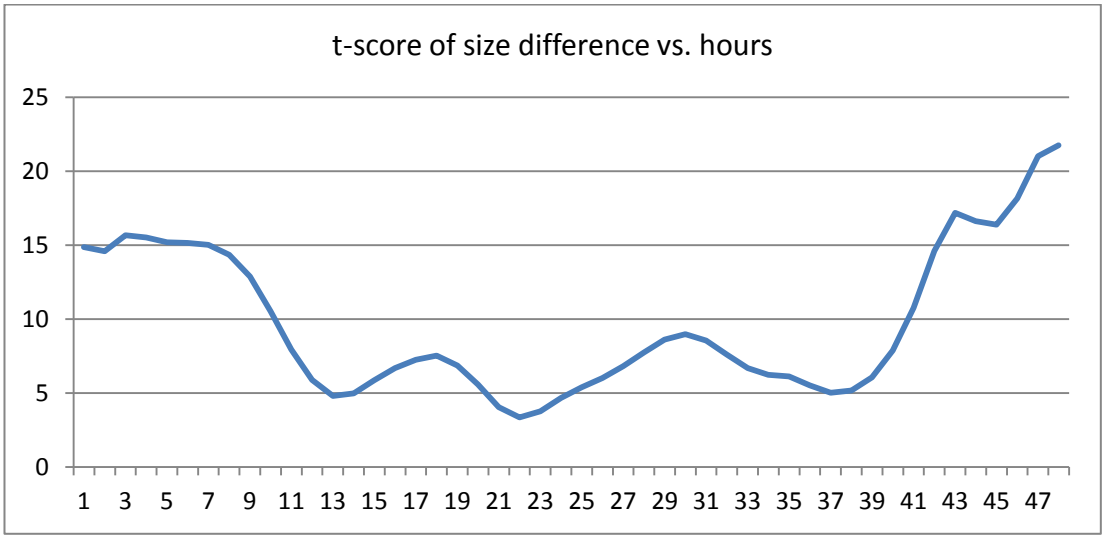

Figure 16. t-score of size difference ((+) Charged Silica NPs, 0.01 Concentration)

Standard deviation of mean uptake rates of hours for silica is given in table below. The negative charge provides slightly more stable uptake rate with smaller standard deviations, when the other variables are constant. Considering only

concentration change, high concentration provides slightly more stable and higher uptake rate.

Table 6. Standard deviation of mean uptake rates for Silica

Type	Silica							
Size	50				100			
Charge	-1		1		-1		1	
Concentration	0.001	0.01	0.001	0.01	0.001	0.01	0.001	0.01
Average of mean uptake rates	0.644	0.737	0.664	0.801	0.703	0.817	0.698	0.742
Standard deviation of mean uptake rates	0.134	0.134	0.152	0.132	0.143	0.130	0.152	0.125

It is also seen from simulation charts that uptake rates in high concentration (1/100) are larger than in low concentration (1/1000) with constant NP size and NP charge. If the NP concentration is low, uptake rate rapidly and decisively goes down soon after. It is also noted that silica shows fewer fluctuations than PMMA.

Simulation results for uptake rates of PLA type of NPs with 250 nm size is given in Figure 15 and 16. There is only one size (250) for PLA nanoparticles. Uptake rates of PLA NPs in high concentration (1/100) graphics are larger than in low concentration (1/1000) graphics, just like silica nanoparticles. In order to prove this, t-test is applied for the difference between means of uptake rates in low and high concentration. The null hypothesis, which is defined as low and high concentration have equal impact, is rejected since t-scores are always less than -2.01; this means that high concentration lead to high uptake rate.

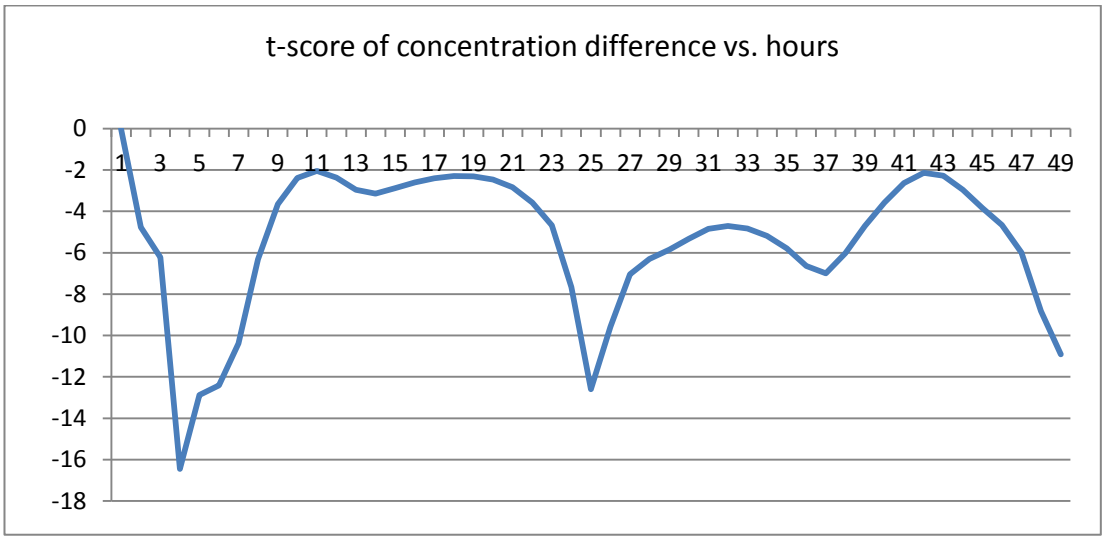

Figure 17. t-score of concentration difference ((-) Charged PLA NPs)

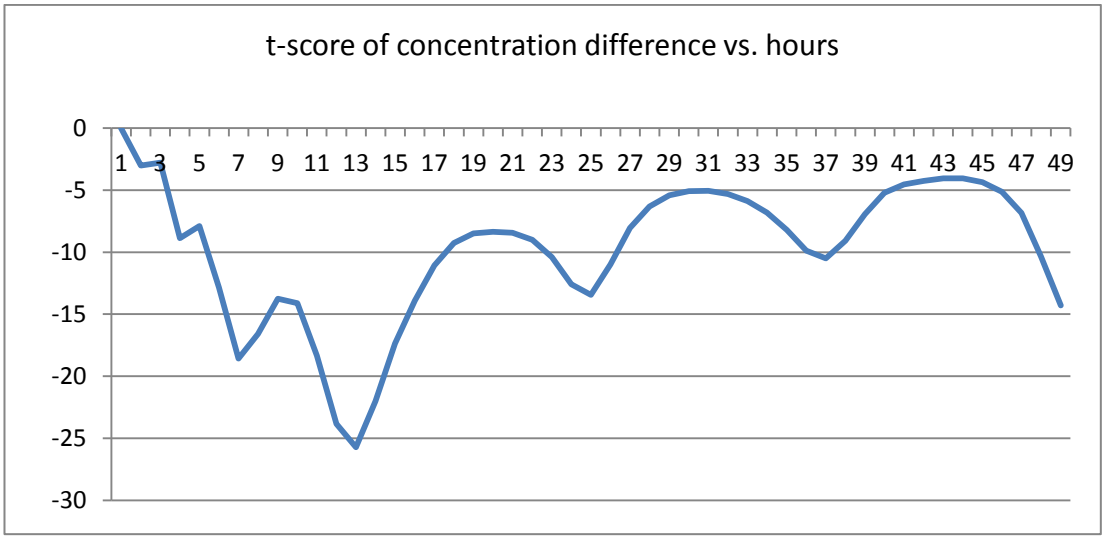

Figure 18. t-score of concentration difference ((+) Charged PLA NPs)

Two-sample t-test is conducted to analyze the effect of charge difference on uptake rate of PLA. According to test results, t-scores are between -2.01 and 2.01 for high concentration; we fail to reject null hypothesis which is defined as negative and positive charges have equal impact. For low concentration, t-scores are

generally between -2.01 and 2.01, so the null hypothesis is mostly accepted. As a result, there is no significant difference between negative and positive charge in general.

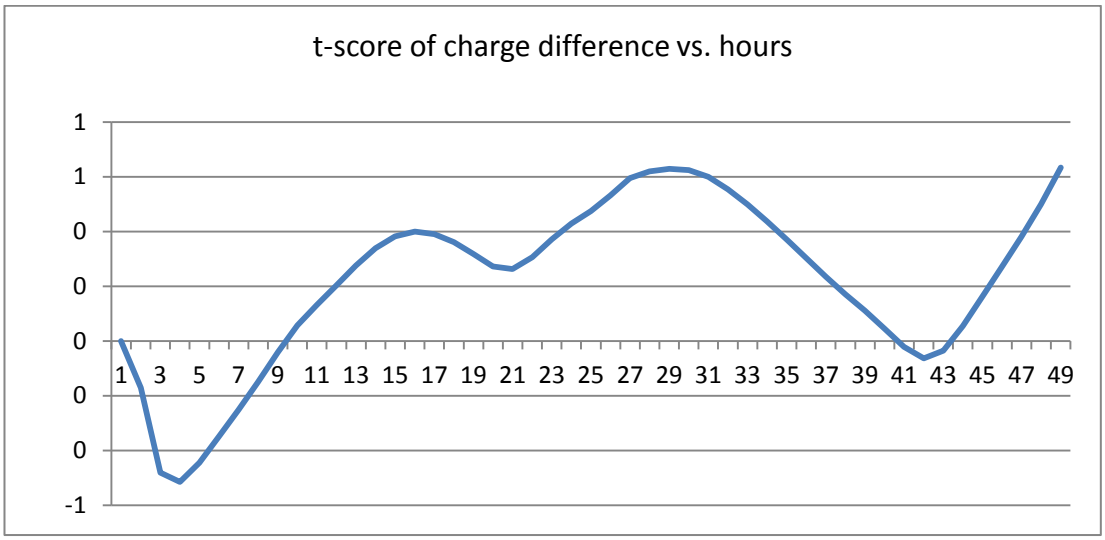

Figure 19. t-score of charge difference (0.01 Concentration PLA NPs)

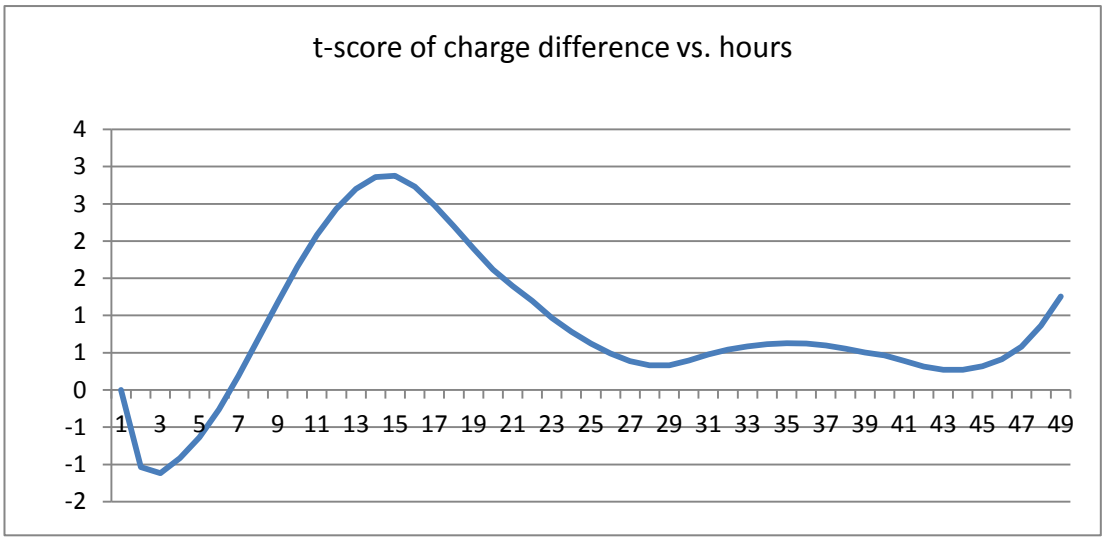

Figure 20. t-score of charge difference (0.001 Concentration PLA NPs)

Standard deviation of mean uptake rates of hours for PLA is given in table below. The (+) charged NPs in low concentration has the smallest standard deviation which leads to slightly more stable uptake rate, but it provides small uptake rate.

Table 7. Standard deviation of mean uptake rates for PLA

Type	PLA			
Size	250			
Charge	-1		1	
Concentration	0.001	0.01	0.001	0.01
Average of mean uptake rates	0.563	0.618	0.505	0.600
Standard deviation of mean uptake rates	0.137	0.138	0.123	0.136

PLA shows fluctuations fewer than PMMA, more than silica. Comparing with the PMMA simulation results, there is no significant difference between PLA and silica results. Size and concentration impact on uptake rate show similar behavior, but a marked difference between PLA and silica is realized due to the surface charge. To generalize these results more accurately, it is necessary to repeat experiments in a wide range of different NP sizes and concentrations.

The results suggest that NPs are most probably transported from the cell membrane via endocytosis, exocytosis, and/or simple diffusion methods. If endocytosis and exocytosis were used mostly, cell integrity could not be preserved and extensive cell death would have occurred after a short period of time due to the reduced membrane, even NP uptake rate would be fixed. However, there is no cell loss during the 48 hours of incubation period. Thus, endocytosis and exocytosis are active transport methods but the dominant method is diffusion; and concentration

difference is the most important factor on diffusion of NPs. It is also distinguished by the simulation results that high concentrations of NPs increase the uptake rate.

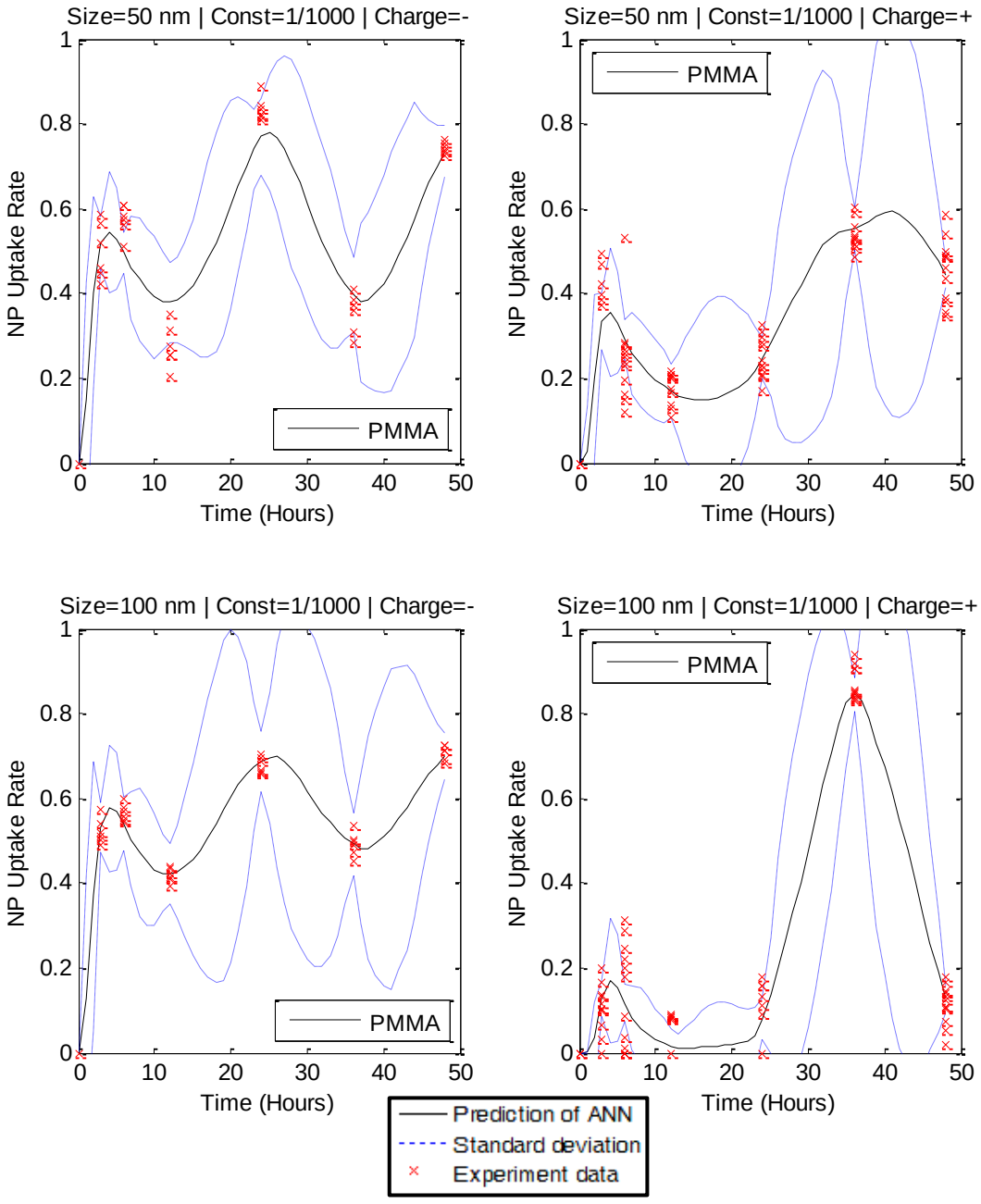

Figure 21. PMMA simulation (Concentration: 1/1000 mg/l)

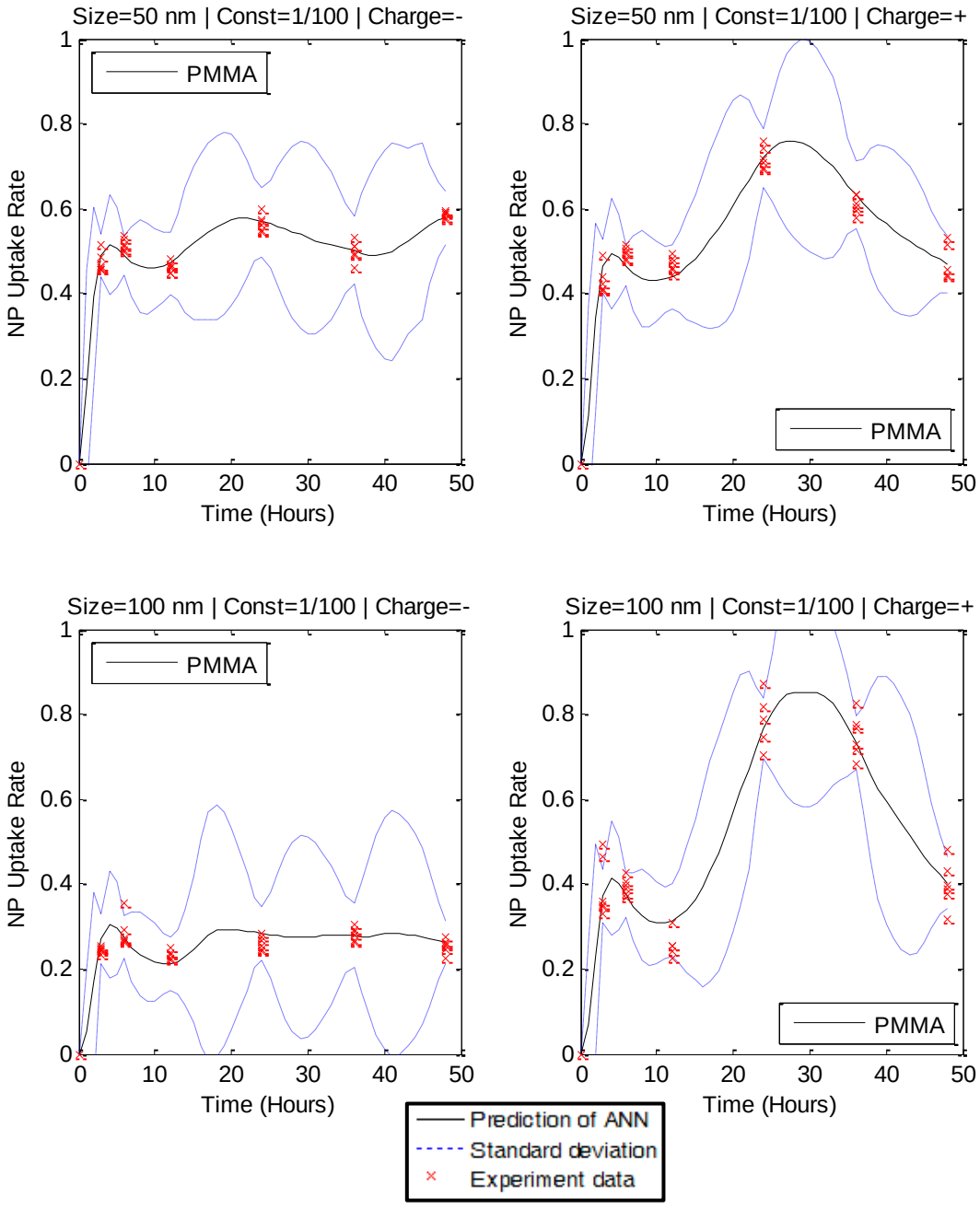

Figure 22. PMMA simulation (Concentration: 1/100 mg/l)

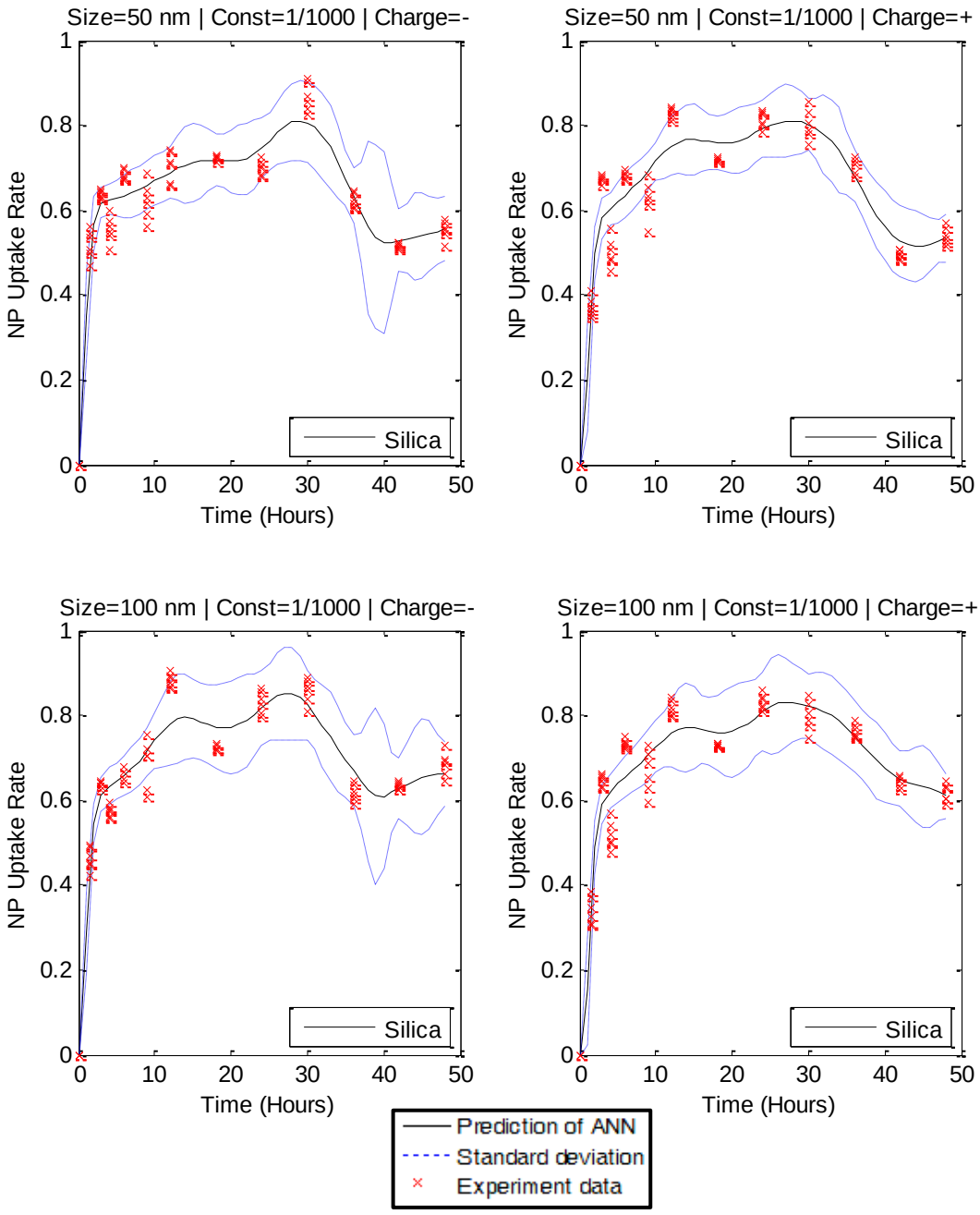

Figure 23. Silica simulation (Concentration: 1/1000 mg/l)

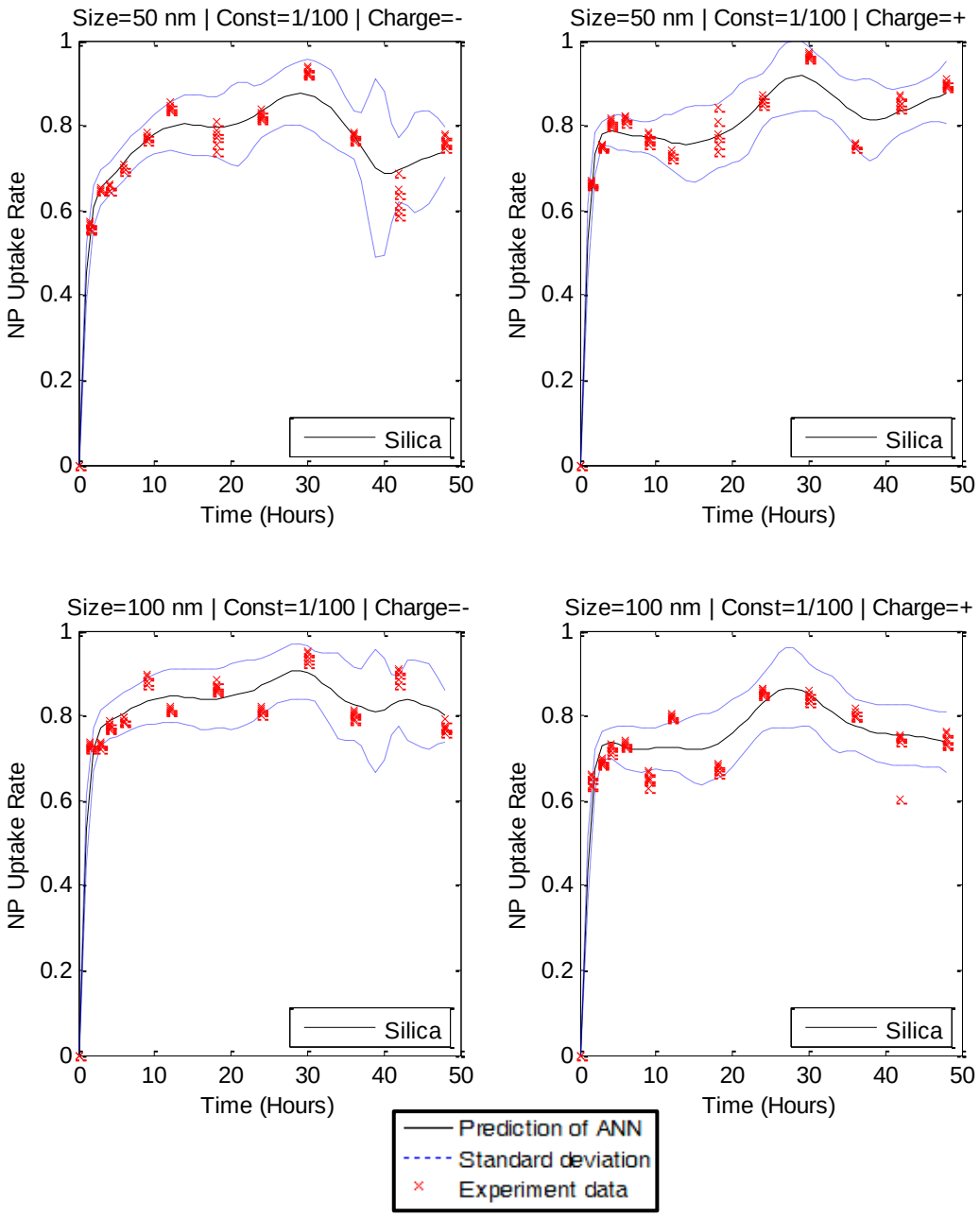

Figure 24. Silica simulation (Concentration: 1/100 mg/l)

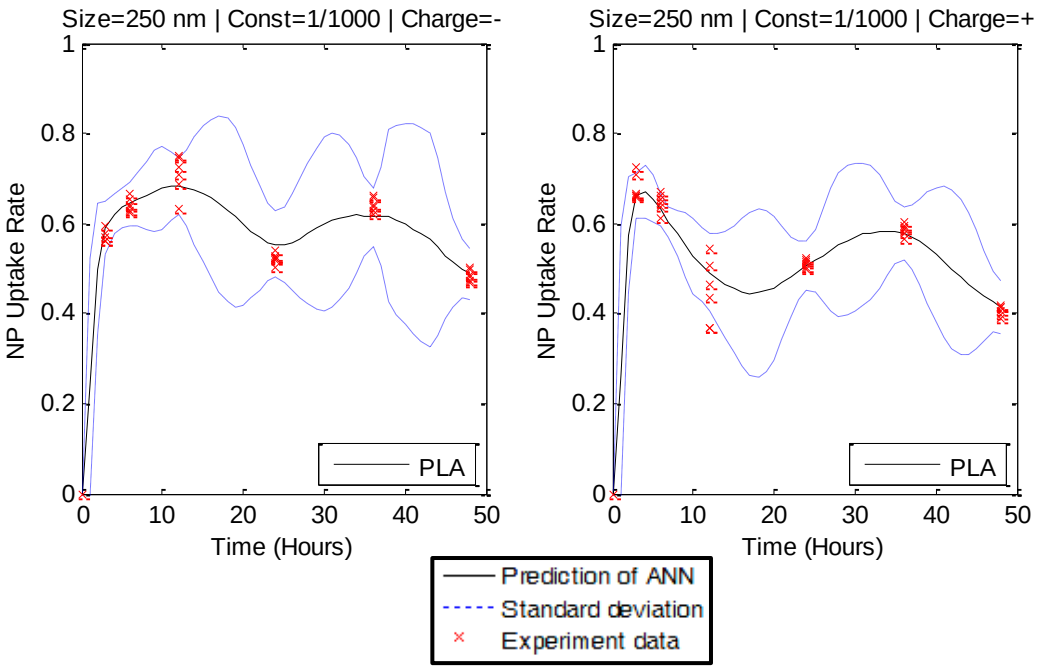

Figure 25. PLA simulation (Concentration: 1/1000 mg/l)

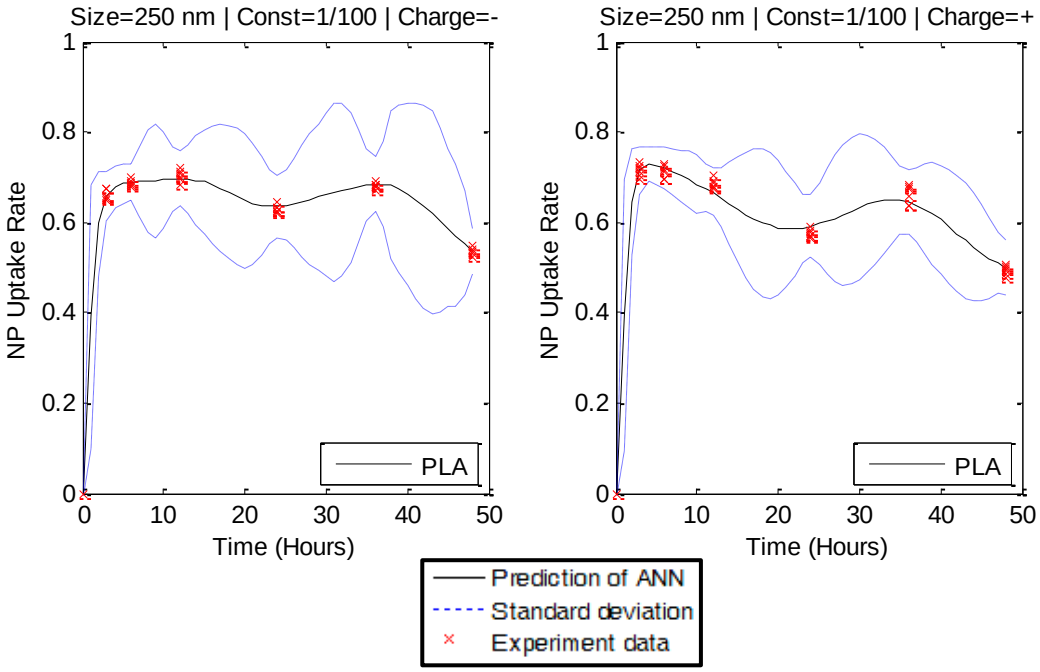

Figure 26. PLA simulation (Concentration: 1/100 mg/l)

Chapter 8

Conclusion

Nanoparticle-cell interactions are investigated for the targeted drug delivery systems, for the treatment of many diseases including cancer. The main objective of this treatment method is to develop nanoparticle structures such that they only go to the targeted cells, release the therapeutic agent and are thrown from the body without toxic effects. Thus, high efficacy of treatment can be provided with fewer amounts of drug dose and systemic side effects minimized.

There are many factors that affect the rate of NPs adhered to the cell surface or entered into the cell. These factors effecting NP uptake rate are the concentration of NPs, surface charge, the chemical structure, shape and size. In order to find the ideal structure of the nanoparticle characterization, NP-cell interactions have to be understood. All the possible NP variations could not be tested experimentally, so it was essential to build a mathematical model. However, such a modeling study is not present in the literature.

This study develops an ANN model for the prediction of cellular NP uptake rate. Several feed forward multilayered ANN models are tested with 14 different

back propagation training algorithms and network structures up to two hidden layers and 20 hidden nodes. The proposed ANN model utilizes the Bayesian regularization training algorithm with single hidden layer and 12 hidden nodes.

The ANN model is simulated for 48 hours to estimate the uptake of NPs for different NP classifications to understand NP-cell interactions. Uptake rates change mostly depending on the type of NP. Silica nanoparticles show fewer fluctuations on uptake rate than PMMA and PLA. Negatively charged NPs have more stable uptake rates than positively charges NPs. Especially, negative surface charge is the most effective factor on uptake rate of PMMA nanoparticles. Uptake rates of PLA and silica are greater in high concentration (1/100) than in low concentration (1/1000). There is no general rule for the effect on uptake rate of 50 or 100 nm sized NPs.

In future work, prediction of NP uptake rate could be modeled by other statistical methods such as multi-linear regression models, additive mix models or support vector machines. The results of other statistical models should be compared and combined with the current study. The proposed ANN model is tested with only in-vitro experiment data. In vivo tissue experiments should be repeated at the level of tissues and organs. In addition, similar experiments should be repeated in different pathological cells and modeled with ANN or other statistical tools.

Bibliography

A. Asati, S. Santra, C. Kaittanis, and J. M. Perez. “Surface-charge-dependent cell localization and cytotoxicity of cerium oxide nanoparticles” ACS Nano, 2010 4(9), 5321–5331.

Ahmed, F.E. “Artificial neural networks for diagnosis and survival prediction in colon cancer.” Molecular Cancer 4(1), 2005, p.29.

Amir Amani, Peter York, Henry Chrystyn, Brian J. Clark, Duong Q. Do, “Determination of factors controlling the particle size in nanoemulsions using Artificial Neural Networks” European Journal of Pharmaceutical Sciences, Volume 35, Issues 1-2, 2 September 2008, Pages 42-51.

B. D. Chithrani, A. A. Ghazani, and W. C. W. Chan “Determining the size and shape dependence of gold nanoparticle uptake into mammalian cells” Nano Letters, 2006, 6(4):662–668.

Boso DP, Lee S, Ferrari M, Schrefler BA, Decuzzi P. “Optimizing particle size for targeting diseased microvasculature: from experiments to artificial neural networks.” Int J Nanomedicine 2011;6:1517-26.

Boyle P. and Levin B. World Cancer Report, Lyon: International Agency for Research on Cancer, 2008.

C. Peetla and V. Labhasetwar “Biophysical characterization of nanoparticle-endothelial model cell membrane interactions” Molecular Pharmaceutics, 2008, 5(3):418–429. PMID: 18271547.

Davda J, Labhasetwar V, “Characterization of nanoparticle uptake by endothelial cells” Int J Pharm 2002, 233:51-59.

Guyton A.C., Hall J. E., “Textbook of Medical Physiology “, Elsevier Saunders, 11th Edition (2006).

Igor Aizenberg and Claudio Moraga. “Multilayer Feedforward Neural Network Based on Multi-valued Neurons (MLMVN) and a Backpropagation Learning Algorithm” Soft Comput.11, 2 (September 2006), p169-183.

J. Lin, H. Zhang, Z. Chen, and Y. Zheng “Penetration of lipid membranes by gold nanoparticles: Insights into cellular uptake, cytotoxicity, and their relationship” ACS Nano, 2010, 4(9), 5421–5429.

Lowery et al. Breast Cancer Research 2009 11:R27

Maciej A. Mazurowski, Piotr A. Habas, Jacek M. Zurada, Joseph Y. Lo, Jay A. Baker, Georgia D. Tourassi, “Training neural network classifiers for medical decision making: The effects of imbalanced datasets on classification performance” Neural Networks, Volume 21, Issues 2-3, March-April 2008, Pages 427-436.

Mark Hudson Beale, Martin T. Hagan, Howard B. Demuth “Neural Network Toolbox - User’s Guide” The Math Works Inc., 2011.

MATLAB - The Language of Technical Computing. 2011. 12 December 2011

Mukta Paliwal, Usha A. Kumar “Neural networks and statistical techniques: A review of applications” Expert Systems with Applications, Volume 36, Issue 1, January 2009, Pages 2-17.

Ne´vine Rizkalla and Patrice Hildgen “Artificial Neural Networks: Comparison of Two Programs for Modeling a Process of Nanoparticle Preparation” Drug Development and Industrial Pharmacy, 2005, 31:1019–1033.

Paulo J. Lisboa, Azzam F.G. Taktak, “The use of artificial neural networks in decision support in cancer: A systematic review” Neural Networks, Volume 19, Issue 4, May 2006, Pages 408-415.

Rumelhart, D. E., Hinton, G. E. & Williams, R. J., "Learning internal representations by error propagation". Parallel Distributed Processing, Cambridge MA: MIT Press, 1986, p318-362.

S. Haykin, “Neural Networks: A Comprehensive Foundation", Second Edition, Prentice-Hall, 1999.

Thomson, R., Sordo, M., OpenClinical: Knowledge Management for Medical Care. “Introduction to Neural Networks in Healthcare”. Harvard (2002).

Xu, S. & Chen, L.(2008) “A Novel Approach for Determining the Optimal Number of Hidden Layer Neurons for FNN’s and Its Application in Data Mining” Proceedings of 5th International Conference on Information Technology and Applications (ICITA 2008), Pp. 683-686.

Zhang Y, Yang M, Portney NG, Cui D, Budak G, Ozbay E, Ozkan M, Ozkan CS., “Zeta potential: a surface electrical characteristic to probe the interaction of nanoparticles with normal and cancer human breast epithelial cells”, Biomed Microdevices. 2008 April; 10(2):321-8.